CONTRACT REPORT ARBRL-CR-00523

AN IMPLICIT NUMERICAL ANALYSIS FOR TWO-DIMENSIONAL TURBULENT INTERIOR BALLISTIC FLOWS

Prepared by

Scientific Research Associates, Inc.
P. O. Box 498
Glastonbury, CT 06033

February 1984

US ARMY ARMAMENT RESEARCH AND DEVELOPMENT CENTER
BALLISTIC RESEARCH LABORATORY
ABERDEEN PROVING GROUND, MARYLAND

Destroy this report when it is no longer needed.
Do not return it to the originator.

Additional copies of this report may be obtained from the National Technical Information Service, U. S. Department of Commerce, Springfield, Virginia 22161.

The findings in this report are not to be construed as an official Department of the Army position, unless so designated by other authorized documents.

The use of trade names or manufacturers' names in this report does not constitute indorsement of any commercial product.

UNCLASSIFIED

SECURITY CLASSIFICATION OF THIS PAGE (When Data Entered)

REPORT DOCUMENTATION PAGE

READ INSTRUCTIONS BEFORE COMPLETING FORM

1. REPORT NUMBER: CONTRACT REPORT ARBRL-CR-00523	2. GOVT ACCESSION NO.
3. RECIPIENT'S CATALOG NUMBER	
4. TITLE (and Subtitle): AN IMPLICIT NUMERICAL ANALYSIS FOR TWO-DIMENSIONAL TURBULENT INTERIOR BALLISTIC FLOWS	5. TYPE OF REPORT & PERIOD COVERED: Final Report Nov. 18, 1981 - May 31, 1982
	6. PERFORMING ORG. REPORT NUMBER
7. AUTHOR(s): Howard J. Gibeling, Henry McDonald	8. CONTRACT OR GRANT NUMBER(s): DAAK11-79-C-0098
9. PERFORMING ORGANIZATION NAME AND ADDRESS: Scientific Research Associates, Inc., P.O. Box 498, Glastonbury, CT 06033	10. PROGRAM ELEMENT, PROJECT, TASK AREA & WORK UNIT NUMBERS
11. CONTROLLING OFFICE NAME AND ADDRESS: US Army AMCCOM, ARDC, Ballistic Research Laboratory, ATTN: DRSMC-BLA-S(A), Aberdeen Proving Ground, MD 21005	12. REPORT DATE: February 1984
	13. NUMBER OF PAGES: 52
14. MONITORING AGENCY NAME & ADDRESS(if different from Controlling Office)	15. SECURITY CLASS. (of this report): UNCLASSIFIED
	15a. DECLASSIFICATION/DOWNGRADING SCHEDULE

16. DISTRIBUTION STATEMENT (of this Report)

Approved for public release; distribution unlimited.

17. DISTRIBUTION STATEMENT (of the abstract entered in Block 20, if different from Report)

18. SUPPLEMENTARY NOTES

19. KEY WORDS (Continue on reverse side if necessary and identify by block number)

Multidimensional Implicit Numerical Method
Two-phase Reacting Flow
Gun Interior Ballistics
Transient Combustion
Time-dependent Adaptive Grid

20. ABSTRACT (Continue on reverse side if necessary and identify by block number)

A two-dimensional implicit interior ballistic computer code (ALPHA) has been developed to solve the turbulent two-phase flow in a gun tube beginning with primer discharge and ending with the projectile exiting the tube. The detailed prediction of flow properties in a gun barrel during firing would aid in the understanding and prevention of both gun barrel erosion and catastrophic gun failures.

The governing partial differential equations and constitutive relations are presented for the two-phase, axisymmetric, turbulent flow in a gun tube with

DD FORM 1 JAN 73 1473 EDITION OF 1 NOV 65 IS OBSOLETE

UNCLASSIFIED

SECURITY CLASSIFICATION OF THIS PAGE (When Data Entered)

a rotating projectile. Results have been obtained for the two-dimensional, two-phase flow in a gun tube with a noncombusting particulate phase. The initial conditions for this case were uniform except for a small gas phase region near the projectile base. The computed results obtained demonstrate the feasibility of making two-dimensional, two-phase predictions for the flow in a gun tube. This procedure also provides a framework for the development and evaluation of two-phase flow turbulence models and constitutive relations which are appropriate for a multidimensional prediction scheme.

TABLE OF CONTENTS

LIST OF FIGURES

LIST OF FIGURES (CONTINUED)

I. INTRODUCTION

A detailed understanding of the phenomena occurring within a gun tube during firing would aid in the development of modern high muzzle velocity gun systems. In particular, the reliable prediction of flow properties in the gun tube would aid in the understanding and prevention of both gun barrel erosion and catastrophic gun failure. The ballistic cycle which we wish to simulate begins with the ignition of the solid propellant particles and ends with the projectile exiting the gun tube and the discharge of hot gases and any unburned propellant. The ignition of the propellant particles is normally initiated by a hot gas-particle flow from a primer consisting of an igniter and a black powder charge. The hot primer gas flows into the propellant bed and heats the propellant particles via conduction, radiation and convection. As the propellant burns gas pressure and temperature rise, thereby promoting the flame spread through the propellant bed. Pressure waves propagate through the chamber, and after the pressure becomes large enough to overcome frictional resistance to motion the projectile will accelerate down the tube. At some point in the cycle the propellant bed will fluidize, and interaction among the particles will diminish. As the projectile moves down the tube several processes may occur which are not considered in the present analysis; these are projectile instability and tube vibration and leakage of propellant gases past the projectile. The former two phenomena would not normally have a significant influence on the two-phase flow in the tube. While leakage of propellant gases may influence the flow especially near the projectile-tube wall juncture, its consideration has been deferred until a later stage of the program development.

Until recently, most other efforts in modeling the flow phenomena in guns have been limited to quasi-one-dimensional, inviscid two-phase flow analyses.[1,2,3,4] Portions of the ballistic cycle can now be modeled with two-dimensional analyses by assuming cylindrically symmetric flow. Gough[5] has developed an inviscid, two-dimensional

1. *P.S. Gough, F.J. Zwarts, "Modeling Heterogeneous Two-Phase Reacting Flow," AIAA Journal, Vol. 17, No. 1, pp. 17-25, 1979.*

2. *K.K. Kuo, J.H. Koo, T.R. Davis, G.R. Coates, "Transient Combustion in Mobile Gas-Permeable Propellants," Acta Astronautica, Vol. 3, pp. 573-591, 1976.*

3. *E.B. Fisher, K.W. Graves, A.P. Trippe, "Application of a Flame Spread Model to Design Problems in the 155 mm Propelling Charge," 12th JANNAF Combustion Meeting, CPIA Pub. 273, Vol. I, pp. 199-219, December 1975.*

4. *H. Krier, S.S. Kokhale, "Modeling of Convective Mode Combustion Through Granulated Propellant to Predict Detonation Transition," AIAA Journal, Vol. 16, No. 2, pp. 177-183, 1978.*

5. *P.S. Gough, "A Two-Dimensional Model of the Interior Ballistics of Bagged Artillery Charges," Paul Gough Associcates, Inc., Report PGA-TR-81-1, Portsmouth, NH, 1981.*

analysis for the ignition phase of the ballistic cycle. The present analysis and computer code ALPHA[6,7] were developed by Scientific Research Associates under Ballistic Research Laboratory sponsorship. This computer code is the first two-phase, two-dimensional, Navier-Stokes analysis to simulate the interior ballistic cycle. A previous paper[8] presented the initial one-phase flow applications of the ALPHA code to the ballistic cycle. These included laminar flow-adiabatic wall, turbulent flow-adiabatic wall and laminar flow-isothermal wall simulations.

This report presents the two-phase, turbulent flow conservation equations (References 6 and 7) and the initial two-dimensional two-phase, nonreacting viscous laminar flow simulation for an idealized ballistic cycle. These two-phase results are compared with a one-phase simulation of the cycle to illustrate the influence of solid particles on the flow development in the tube.

II. GOVERNING EQUATIONS

The governing equations for a two-phase, two-dimensional flow in a gun tube have been presented previously in References 6 and 7. Since the large number of propellant particles present precludes treating each individually, the present formulation considers averaged flow properties. These equations (References 6 and 7) were obtained using the formal averaging procedure presented by Gough[9,10] and Gough and Zwarts (Reference 1), with extensive reference to the time-

6. *H. J. Gibeling, R.C. Buggeln and H. McDonald, "Development of a Two-Dimensional Implicit Interior Ballistics Code," US Army ARRADCOM/Ballistic Research Laboratory, Contract Report ARBRL-CR-00411, Aberdeen Proving Ground, MD, January 1980 (AD A084092).*

7. *H.J. Gibeling and H. McDonald, "Development of a Two-Dimensional Implicit Interior Ballistics Code," US Army ARRADCOM/Ballistic Research Laboratory, Contractor Report ARBRL-CR-00451, Aberdeen Proving Ground, MD, March 1981 (AD A100276).*

8. *J.A. Schmitt, N.E. Banks, C.K. Zoltani, H.J. Gibeling and T.L. Mann, "Two-Phase Viscous Flow Modeling of Interior Ballistics, Algorithm and Numerical Predictions for an Idealized Lagrange Gun," Proceedings of the ASME Symposium on Computers in Flow Predictions and Fluid Dynamic Experiments, Edited by K.N. Ghia, T.J. Mueller and B.R. Patel, pp. 181-190, 1981.*

9. *P.S., Gough, "Derivation of Balance Equations for Heterogeneous Two-Phase Flow by Formal Averaging," ARO Workshop on Multiphase Flows, USA Ballistic Research Laboratory, pp. 71-80, February 1978.*

10. *P.S. Gough, "The Flow of a Compressible Gas Through an Aggregate of Mobile, Reacting Particles," Ph.D Thesis, Department of Mechanical Engineering, McGill University, Montreal, 1974.*

averaging approach of Ishii.[11] In this approach an averaged variable is the space-time integral of the product of the local variable and a weighting function which reflects the influence of remote points on the average values. The local equations are replaced by a set of averaged equations in the averaged variables for each spatial position and time. The two phases are treated distinctly in this so-called two-fluid model with momentum, mass and energy exchange terms between the two phases being replaced by appropriate constitutive relations. The governing partial differential equations and constitutive relations used in the present analysis are given in the Appendix.

The governing equations in the ALPHA code were formulated in conservation form by application of a Jacobian transformation to the equations in cylindrical-polar coordinates (Reference 7). A consistent technique for determination of the local time-dependent Jacobian determinant of the coordinate transformation was implemented to reduce geometrical errors in computed results. An axisymmetric time-dependent adaptive coordinate system for interior ballistics flow field calculations is utilized, with the projectile and any distinct filler elements treated using a quasi-one-dimensional lumped parameter analysis. The governing equations, constitutive relations, and the time-dependent coordinate system have been incorporated into an existing computer code which solves the multidimensional time-dependent compressible Navier-Stokes equations using a consistently split, linearized, block-implicit (LBI) numerical scheme developed by Briley and McDonald.[12,13] Since the LBI algorithm is well documented in References 12 and 13, it will not be discussed further here.

III. TWO-PHASE FLOW MODEL PROBLEM

Because of the complex nature of the multidimensional, two-phase flow phenomena occurring in a gun tube, an idealized two-phase flow in a Lagrange gun has been simulated. This problem permits verification of the two-phase equation system in the ALPHA code and provides an understanding of some basic two-phase flow mechanisms which occur in a real gun. The Lagrange gun is a smooth tube of constant radius which is closed at one end by the breech. The model combustion chamber is bounded by the breech, a flat based projectile, and the tube wall. The chamber is filled initially with a high pressure, high temperature gas-particle mixture with a small gas-phase region adjacent to the

11. *M. Ishii, Thermo-Fluid Dynamic Theory of Two-Phase Flow, Eyrolles, Paris, 1975.*

12. *W.R. Briley and H. McDonald, "Solution of the Multidimensional Compressible Navier-Stokes Equations by a Generalized Implicit Method," Journal of Computational Physics, Vol. 24, No. 4, pp. 372-397, 1977.*

13. *W.R. Briley and H. McDonald, "On the Structure and Use of Linearized Block Implicit Schemes," Journal of Computational Physics, Vol. 34, No. 1, pp. 54-73, 1980.*

projectile base. In the present case, the particles were chosen to be spherical with a constant 0.1 mm diameter throughout. No combustion of the particles is permitted in this calculation, so that this simulation of the ballistic cycle approximately represents that of a real gun if the propellant combustion ceases before the projectile begins moving at time t = 0. As in prior one-phase Lagrange gun simulations (Reference 8), frictional forces between the projectile and the tube wall are neglected. For this initial two-phase simulation the flow is assumed to remain laminar throughout the cycle, and an adiabatic wall condition is applied. Even though the actual flow in a gun tube is turbulent and the heat transfer to the walls influences the flow field, the present simulation provides insight into the effects of solid particles on the viscous flow development in the tube. The required governing equations are the gas and solid phase continuity and momentum conservation equations, gas phase energy conservation equation and the solid phase heat conduction equation. Heat transfer between the gas and solid phases is accomplished by the interphase heat transfer coefficient model with the particle surface temperature advanced in time after the coupled solution of the gas and solid phase continuity and momentum equations and the gas phase energy equation. However, the test case was run with thermally insulated particles, i.e., no heat transfer between the gas and solid phase was permitted and the particle internal energy remained constant throughout the cycle. The particle size is assumed to remain constant, and the gas phase specific heat (at constant pressure) and mixture molecular weight are also assumed to remain constant throughout the cycle. The Nobel-Abel equation of state, Sutherland's laws for viscosity and thermal conductivity, and the Fourier heat conduction relation are employed for the gas phase.

The following coupled boundary conditions are utilized for the two-phase calculation: at the breech, projectile and tube wall, no-slip conditions are imposed on the gas phase velocities and the gas phase density is determined from the normal momentum equation. At the solid surfaces, the adiabatic condition of zero normal derivative of gas temperature is applied. At the breech and tube wall, the normal component of solid phase velocity is assumed to be zero, while the tangential component is determined by assuming that there is no solid phase momentum decrease due to interaction with the wall. This latter condition is approximated by assuming a zero normal derivative of the solid phase tangential velocity component. The solid phase partial density (related to void fraction) at the breech is obtained by application of the solid phase continuity equation and at the tube wall is obtained by assuming a zero normal derivative of solid phase partial density. At the projectile base, the solid phase velocity and partial density are set to zero (unit void fraction) since there is only gas present at that location. At the tube centerline, the symmetry conditions of zero radial velocities and zero radial derivatives of all other variables are imposed.

The computational mesh employed in the calculations consists of 61 uniformly spaced mesh points in the axial direction and 19 nonuniformly spaced mesh points in the radial direction. The mesh points are concentrated near the tube wall in the radial direction in order to resolve the gas phase boundary layer; the first point is at the tube

centerline (10 mm from the wall), the tenth is 0.306 mm from the wall, the seventeenth is 7.56 μm from the wall, and the nineteenth point is at the wall. The gun tube configuration, gas and solid phase properties, and initial conditions for the calculation are given in Table 1.

TABLE 1. TWO-PHASE LAGRANGE GUN PARAMETERS

Bore Diameter	20mm
Combustion Chamber Length	0.175m
Total Bore Length	1.290m
Projectile Mass	0.120kg
Gas Molar Mass	23.8g/mole
Covolume	$1.08 \cdot 10^{-3}$ m^3/kg
Ratio of Gas Specific Heats	1.271
Solid Particle Diameter	0.1mm
Particle Density	1500 kg/m^3
Initial Gas Pressure	$300 \cdot 10^6$ Pa
Initial Gas Temperature	3000 K
Initial Void Fraction; $0 \leq Z \leq 0.169m$	0.94
$0.169 < Z < 0.175m$	1.0

A one-phase flow Lagrange gun simulation was computed with nearly the same computational mesh (19 x 49) for comparison with the two-phase calculation. The additional grid points in the axial direction were used in the two-phase calculation because of the large void fraction gradient occurring near the projectile base. The one-phase simulation has the same parameters as Table I except, of course, that the void fraction is unity throughout. As previously reported by Schmitt et al (Reference 8), the one-phase Lagrange gun results compare favorably with both a one-dimensional analytic isentropic solution[14] which is valid for early times in the cycle and the numerical calculation of Heiser and Hensel.[15] A one-phase calculation run with the present computer code was compared to an identical calculation run with the code utilized by Reference 8 in order to verify the present one-phase results. These results give confidence that the numerical procedure is capable of capturing the pressure waves propagating in the gun tube as long as the spatial and temporal resolution remain adequate.

The two-phase calculation was started with a time step of 2.0 μs, and the time step was permitted to increase to maintain a predetermined maximum change in the solution over each time step. The maximum time step reached in this case was about 4.3 μs. The one-phase calculation was run with a constant time step of 5.0 μs, so that temporal accuracy in the two cases should be comparable. The calculations were both terminated at muzzle exit time. The results are compared shortly before muzzle exit time with the projectile speed, position, and problem time of 581 m/s, 1.282 m, and 2.575 ms, respectively, for the one-phase simulation and 559 m/s, 1.289 m, and 2.673 ms, respectively, for two-phase simulation. The one-phase calculation was actually run in the two-phase mode with near unity void fraction (0.999999), but solving only the gas-phase conservation equations. The one-phase calculation required 518 time steps and 0.82 hours of CP time on the BRL CDC 7600 with the 19 x 49 mesh and 4 coupled equations; the two-phase calculation required 891 time steps and 3.06 hours of CP time with the 19 x 61 mesh and 7 coupled equations.

The comparison of the boundary layer development in the one-phase and two-phase cases shows some interesting results. The boundary layer axial velocity profiles are shown in Figures 1 through 4, for several axial positions, from which it is seen that the gas velocities are smaller in the two-phase case than in the one-phase case, reflecting the energy expended to accelerate the solid particles. The solid phase lags behind the gas in the core flow as expected; the particle velocity decreases very little near the wall because of the relatively large particle

14. *E.H. Love and F.B. Pidduck, "Lagrange's Ballistic Problem," Phil. Trans. Roy. Soc., Vol. 222, pp. 167-226, 1921-22.*

15. *R. Heiser and D. Hensel, "Berechnung der Gasströmung in einem Waffenrohr mit Hilfe des Zweidimensionalen AMI-Modells," E1/81, Ernest-Mach-Institut, Abteilung für Ballistik, Weil am Rhein, West Germany, January 1981.*

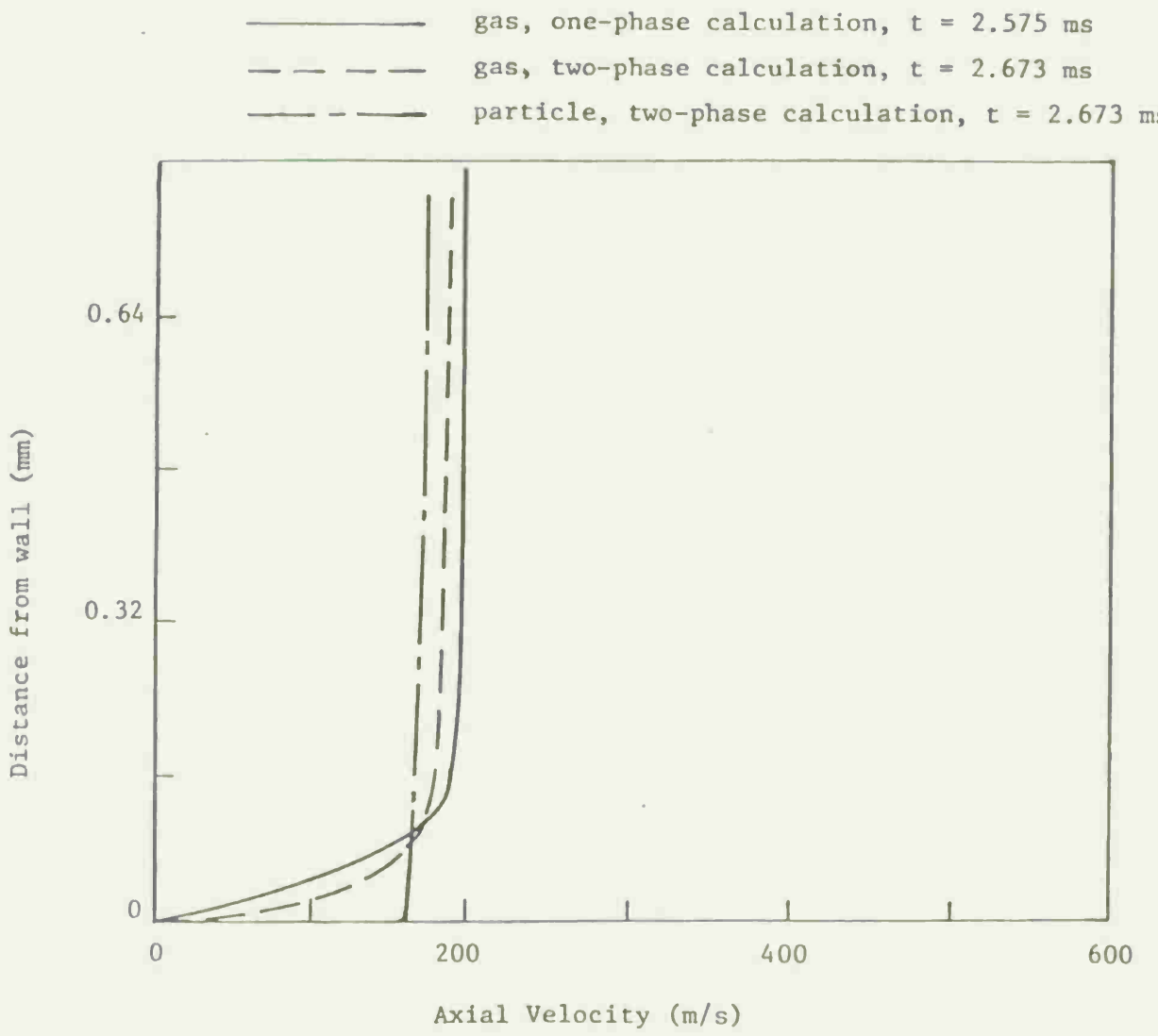

Figure 1 - Comparison of one- and two-phase tube wall boundary layer profiles at muzzle exit time for Z = 0.43 m.

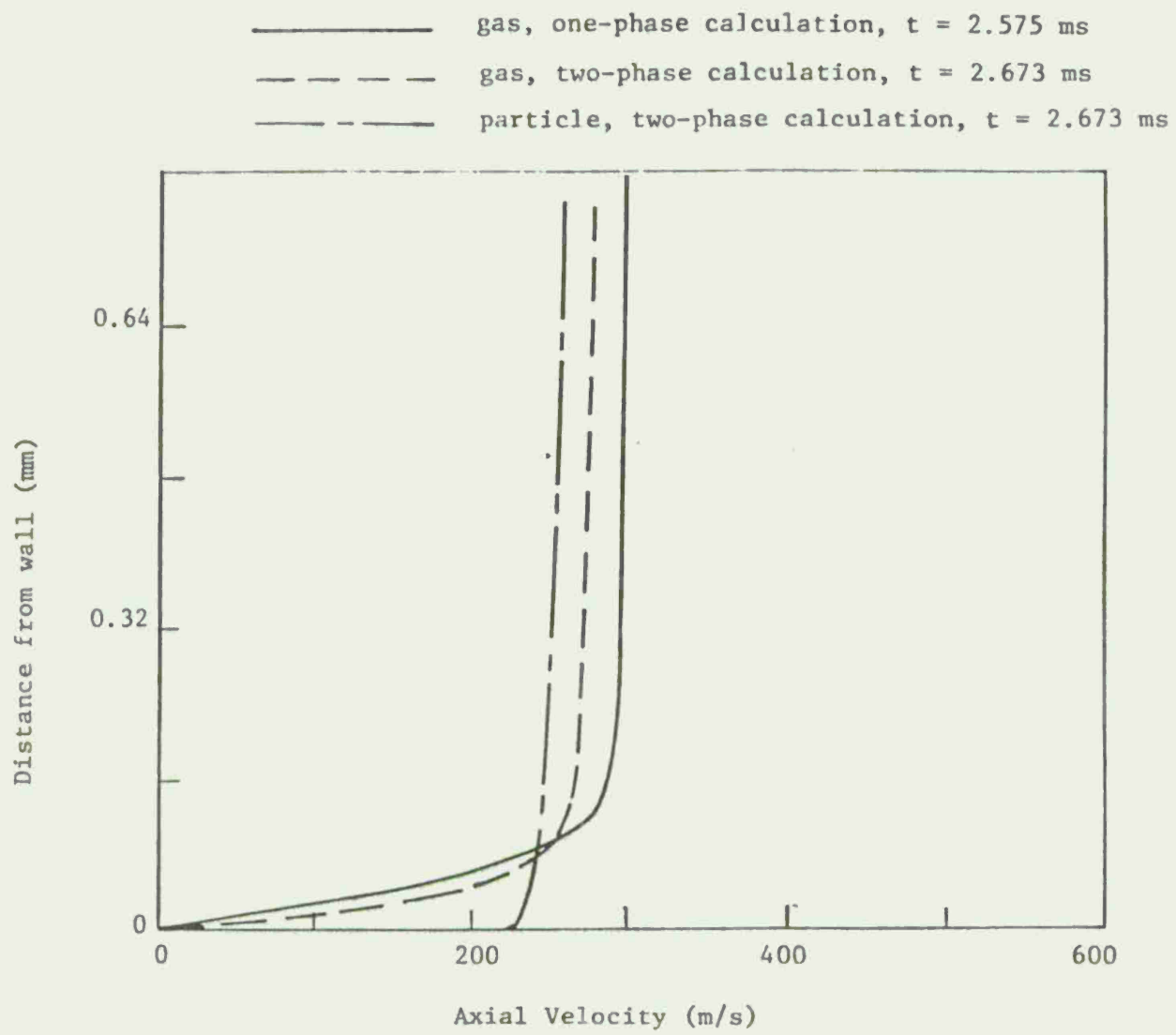

Figure 2 - Comparison of one- and two-phase tube wall boundary layer profiles at muzzle exit time for Z = 0.64 m.

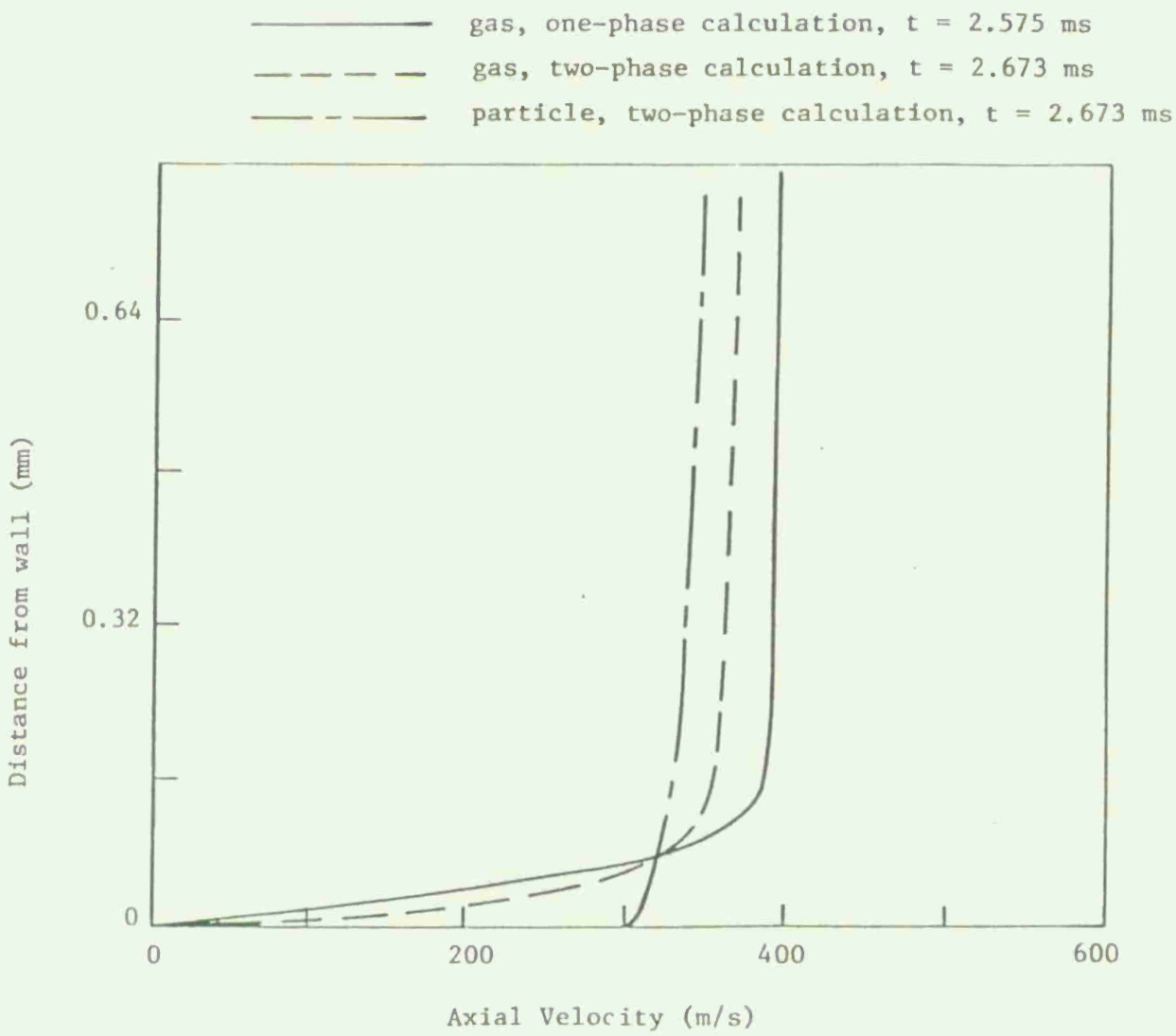

Figure 3 - Comparison of one- and two-phase tube wall boundary layer profiles at muzzle exit time for Z = 0.86 m.

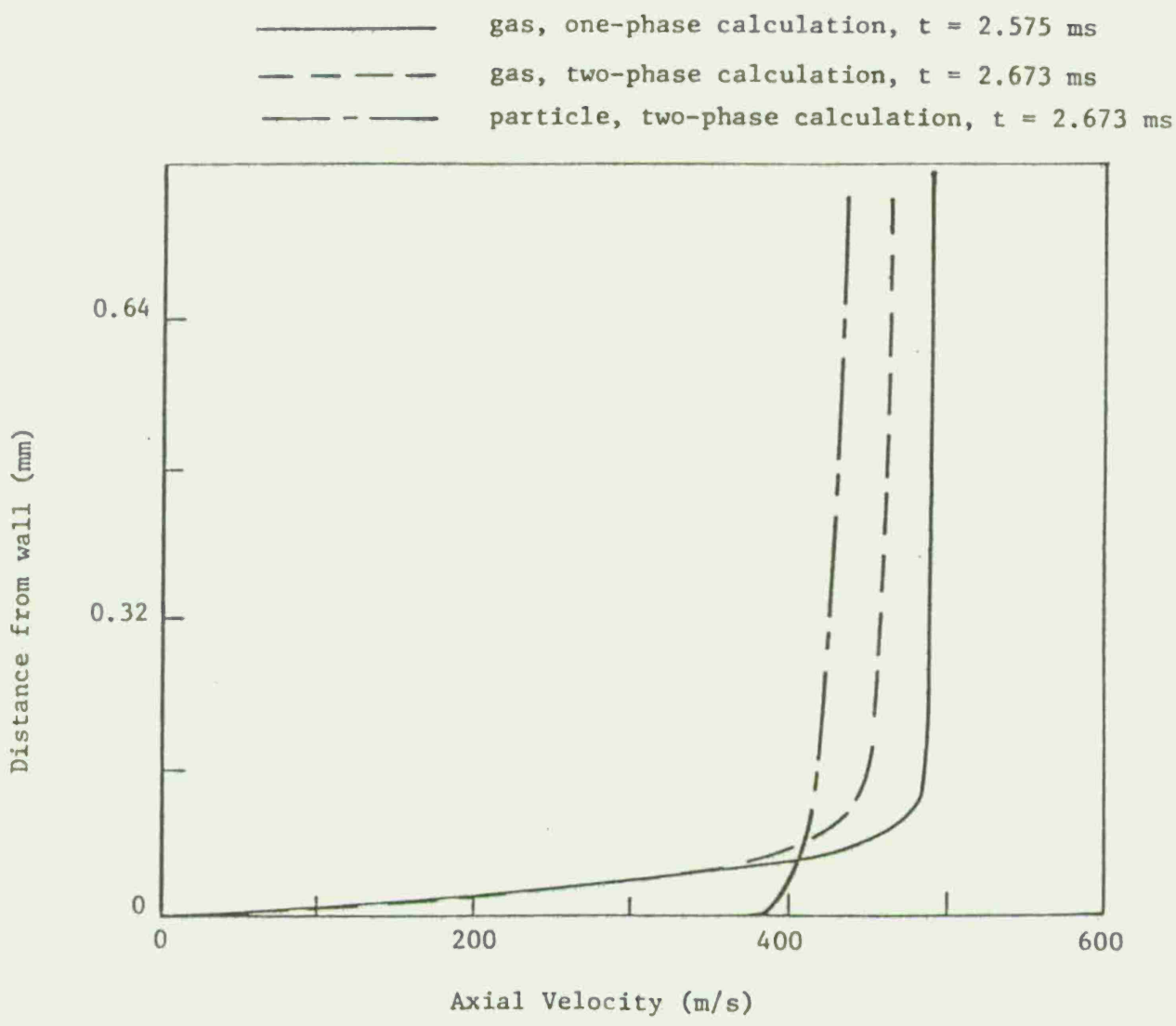

Figure 4 - Comparison of one- and two-phase tube wall boundary layer profiles at muzzle exit time for Z = 1.07 m.

size and the assumption of no particle momentum loss at the wall. The transverse velocity profiles across the entire tube are shown in Figures 5 through 8 for the same axial positions as in Figures 1 through 4. The transverse velocities are quite small compared to the axial velocities for this relatively simple case. Also, the velocities near the juncture of the tube wall and the projectile base are strongly influenced by the treatment of that point. In the present calculations a perfect seal was assumed so that this corner juncture is a singular point. In order to obtain more accurate predictions in the corner region, the gap region between the tube wall and the projectile may have to be included in the computational domain. The positive radial velocities (toward the tube wall) observed near the projectile base (Figure 8) are expected on physical grounds. However, it has been observed that the quantitative results near the projectile base are sensitive to the axial grid spacing,[16] so that a locally refined mesh should be utilized in that region.

The character of the tube wall boundary-layer is noticeably different in the one- and two-phase cases, as seen in Figures 1 through 8. The axial distribution of boundary layer displacement thickness (Figure 9) gives another indication of the influence of solid particles on the wall boundary layer. Here, the displacement thickness (δ^*) is

$$\delta^*(z,t) = \int_0^R \left[1 - \frac{\rho(r,z,t)\, w(r,z,t)}{\rho_c(z,t)\, w_c(z,t)} \right] \frac{r}{R}\, dr \qquad (1)$$

where the subscript c denotes the centerline value, w is the axial gas velocity, ρ is the gas density, and R is the tube radius. It can be seen that the displacement thickness is larger in the two-phase case for most of the distance from the projectile to the breech. Furthermore, the wall shear stress is larger in the two-phase case. If the thermal boundary layer for a flow with wall heat transfer exhibits similar behavior, an increase in wall heat flux would be expected due to the presence of solid particles of the present size.

The void fraction distribution shown in Figure 10 illustrates the increase in thickness of the gas zone ($\alpha = 1.0$) near the projectile; however, this is essentially a one-dimensional process since no particle momentum loss at the wall has been assumed and the particle size is the same order as the boundary layer thickness. Since the particle size is comparable to the gas boundary layer thickness, the interphase correlations must be examined to include near-wall effects and a particle-wall interaction model should be developed to account for particle momentum transfer to the wall. The axial distribution of velocities for the one- and two-phase calculations are compared in Figures 11 through 13. The

16. *J.A. Schmitt and T.L. Mann, "Calculation of the Compressible Flow in the Lagrange Gun by the Interior Ballistics Algorithm Alpha," Proceedings of the DEA-G-1060 Meeting, Eglin Air Force Base, October 1980.*

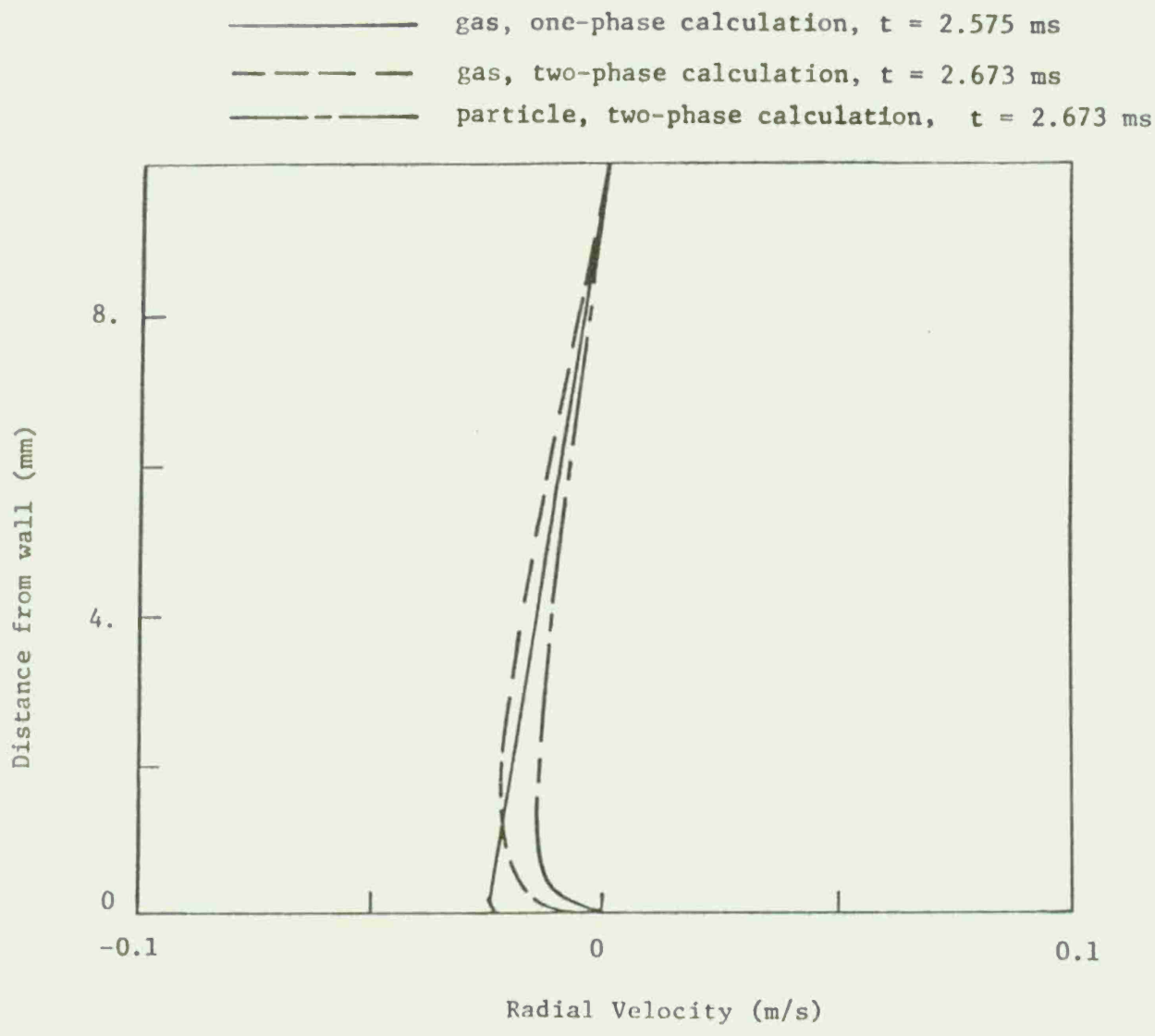

Figure 5 - Comparison of one- and two-phase radial velocity profiles at muzzle exit time for Z = 0.43 m.

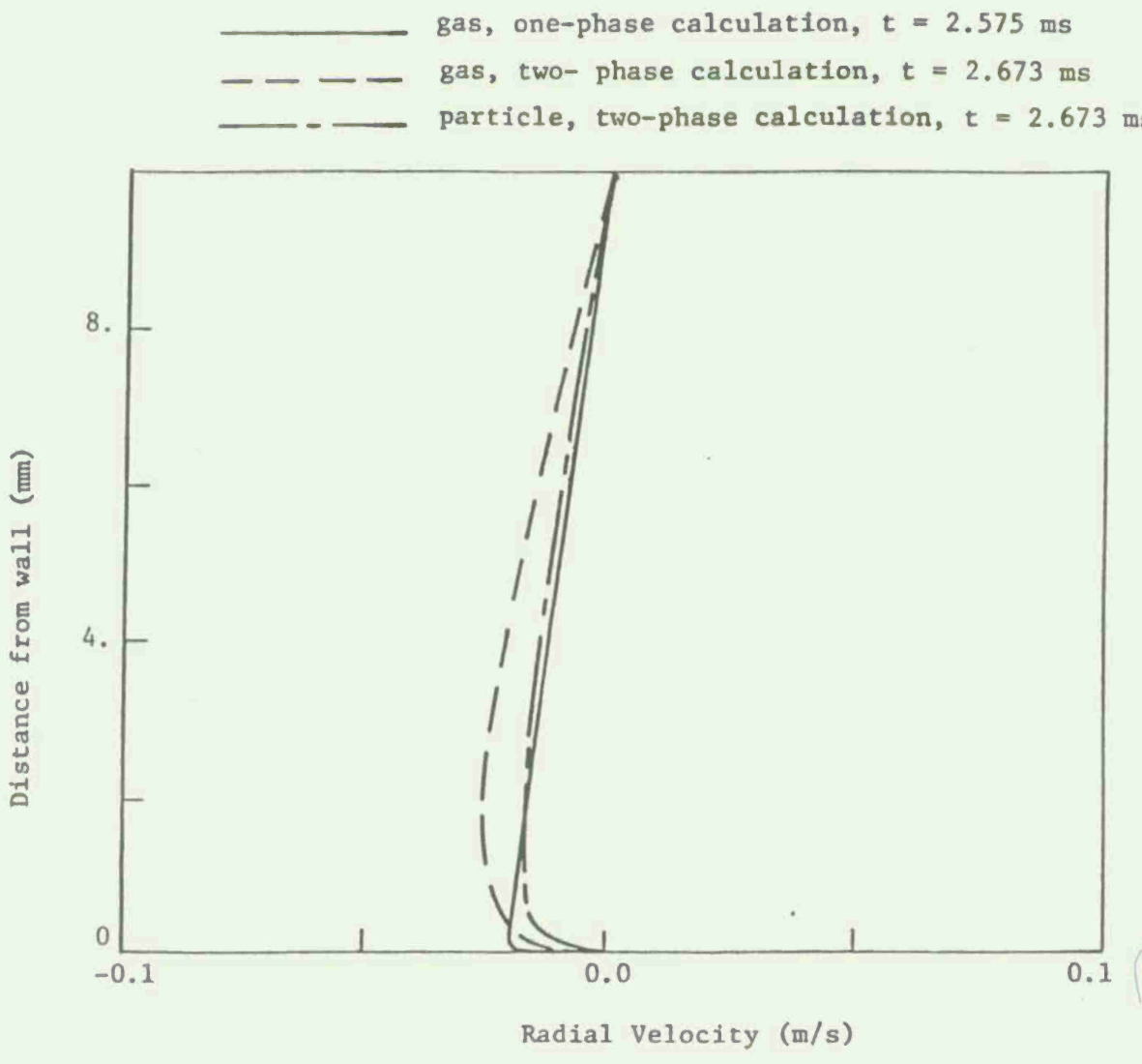

Figure 6 - Comparison of one- and two-phase radial velocity profiles at muzzle exit time for Z = 0.64 m.

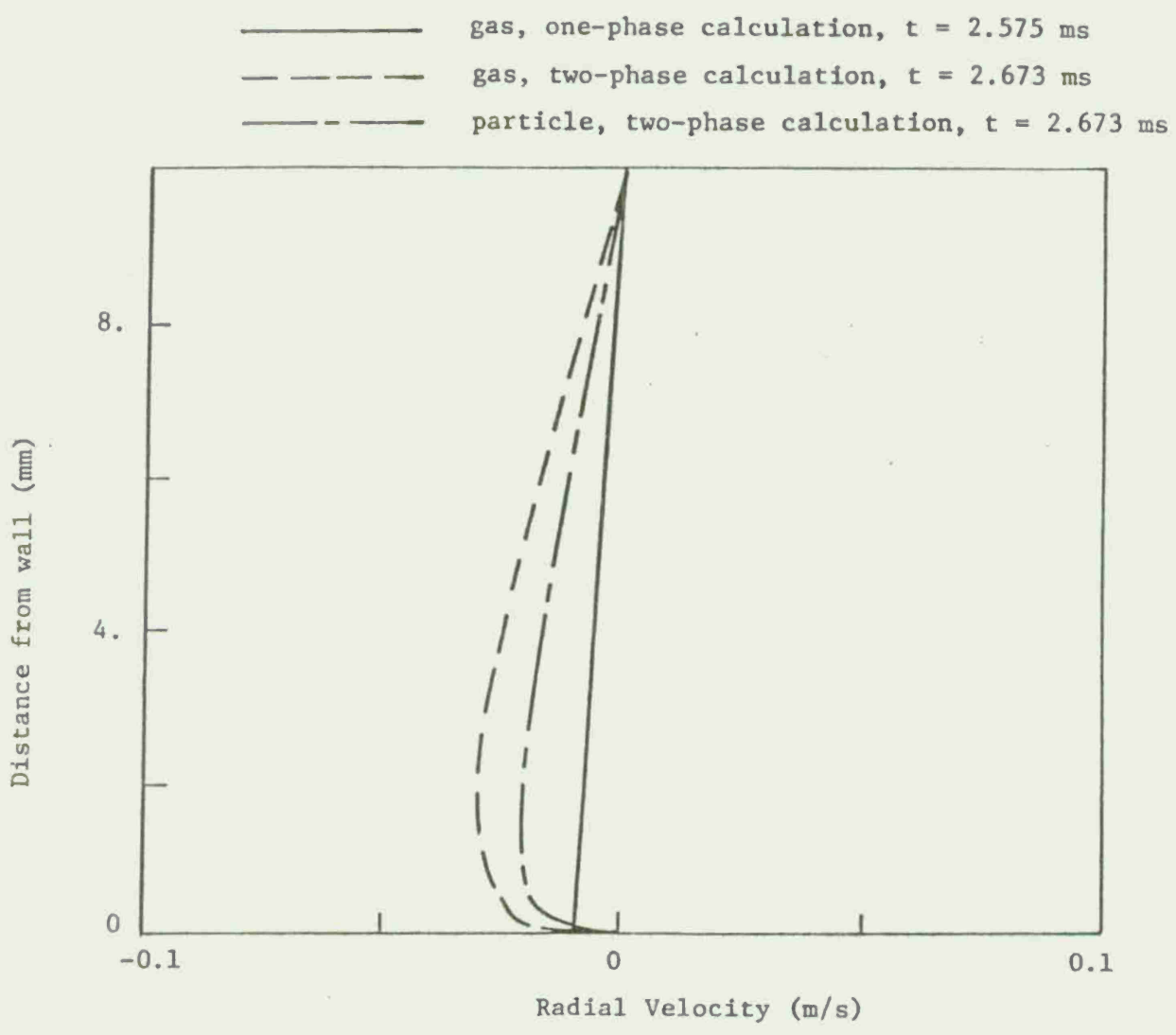

Figure 7 - Comparison of one- and two-phase radial velocity profiles at muzzle exit time for Z = 0.86 m.

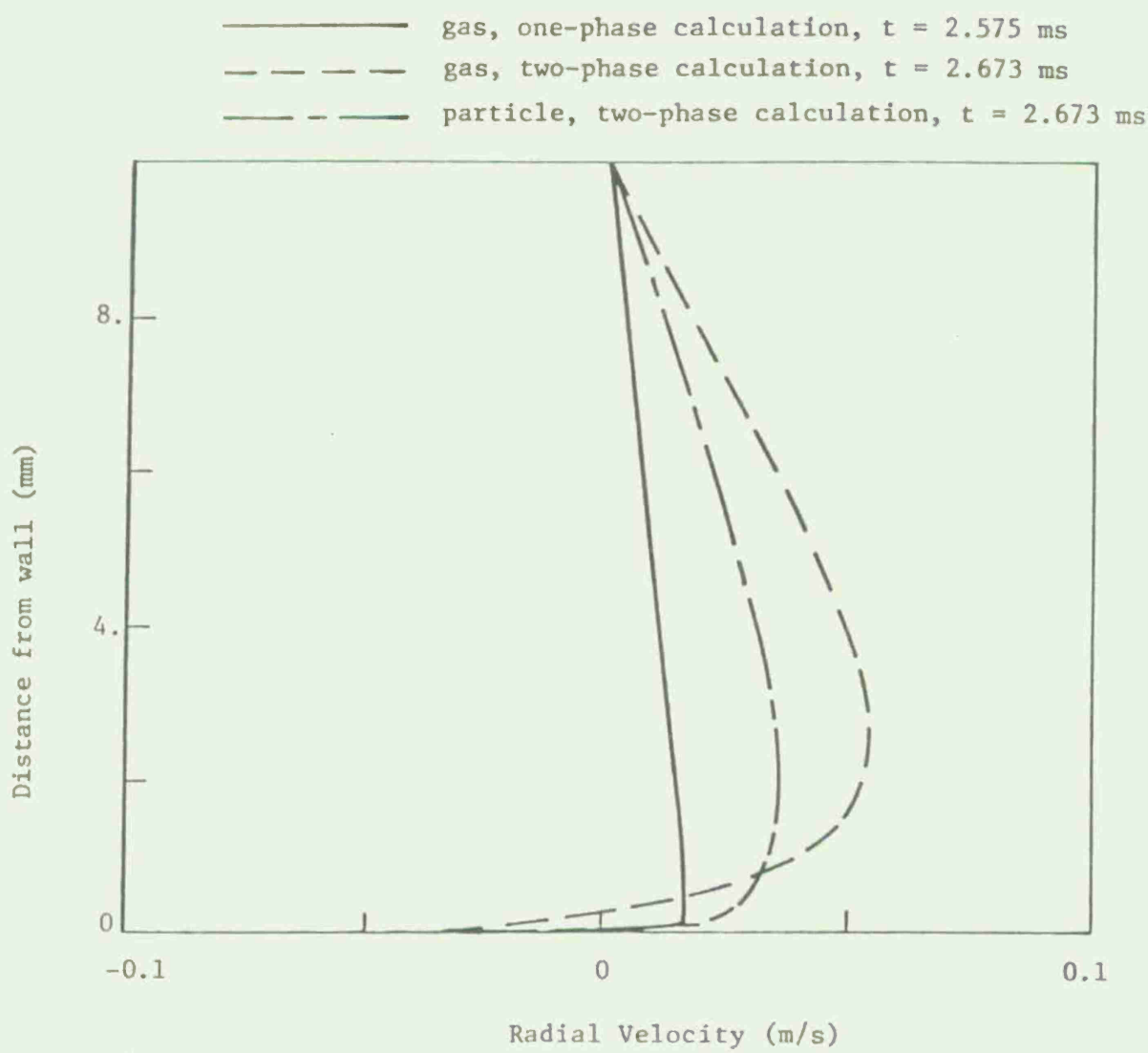

Figure 8 - Comparison of one- and two-phase radial velocity profiles at muzzle exit time for Z = 1.07 m.

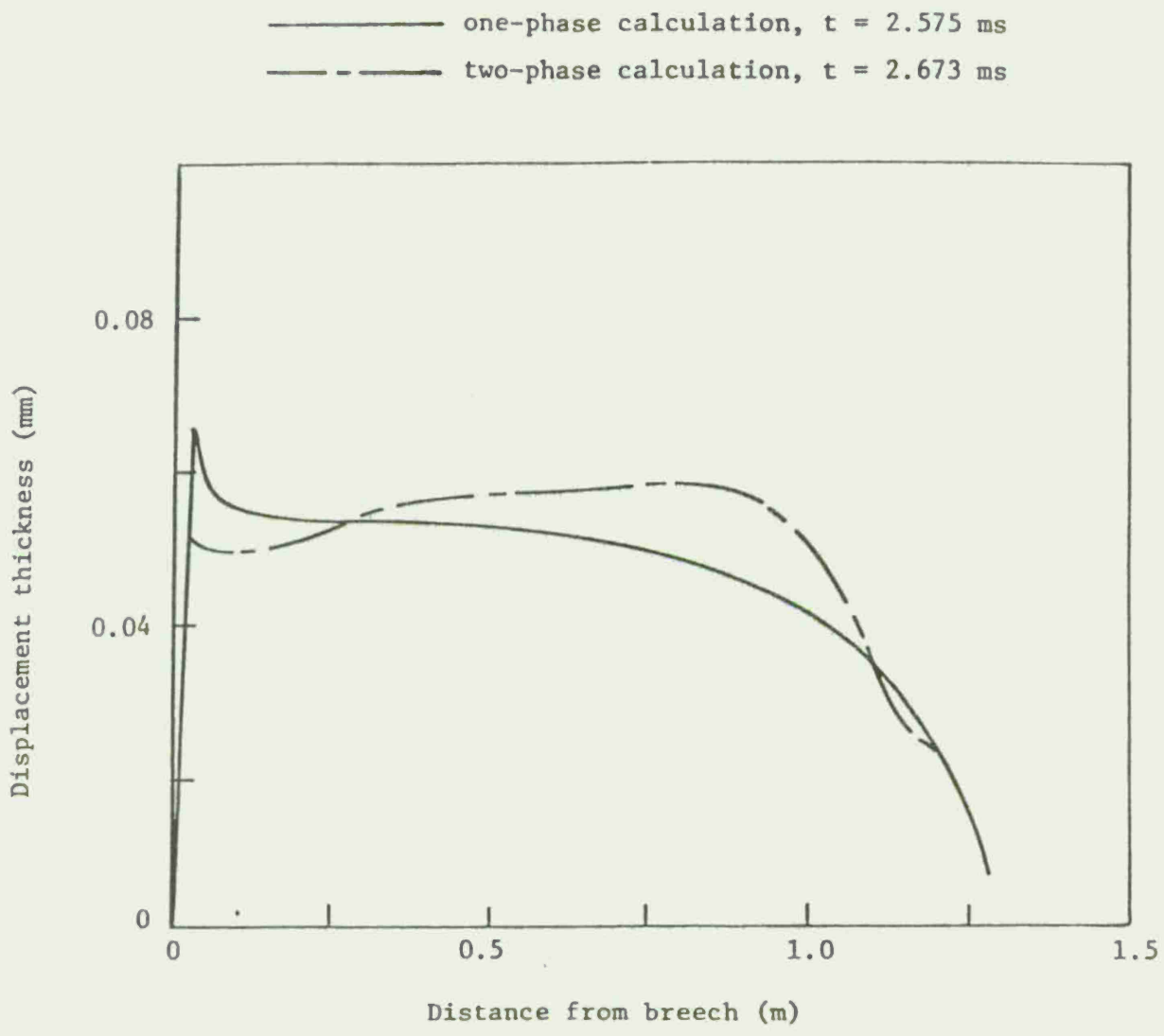

Figure 9 - Comparison of boundary layer displacement thickness for one- and two-phase calculations at muzzle exit time.

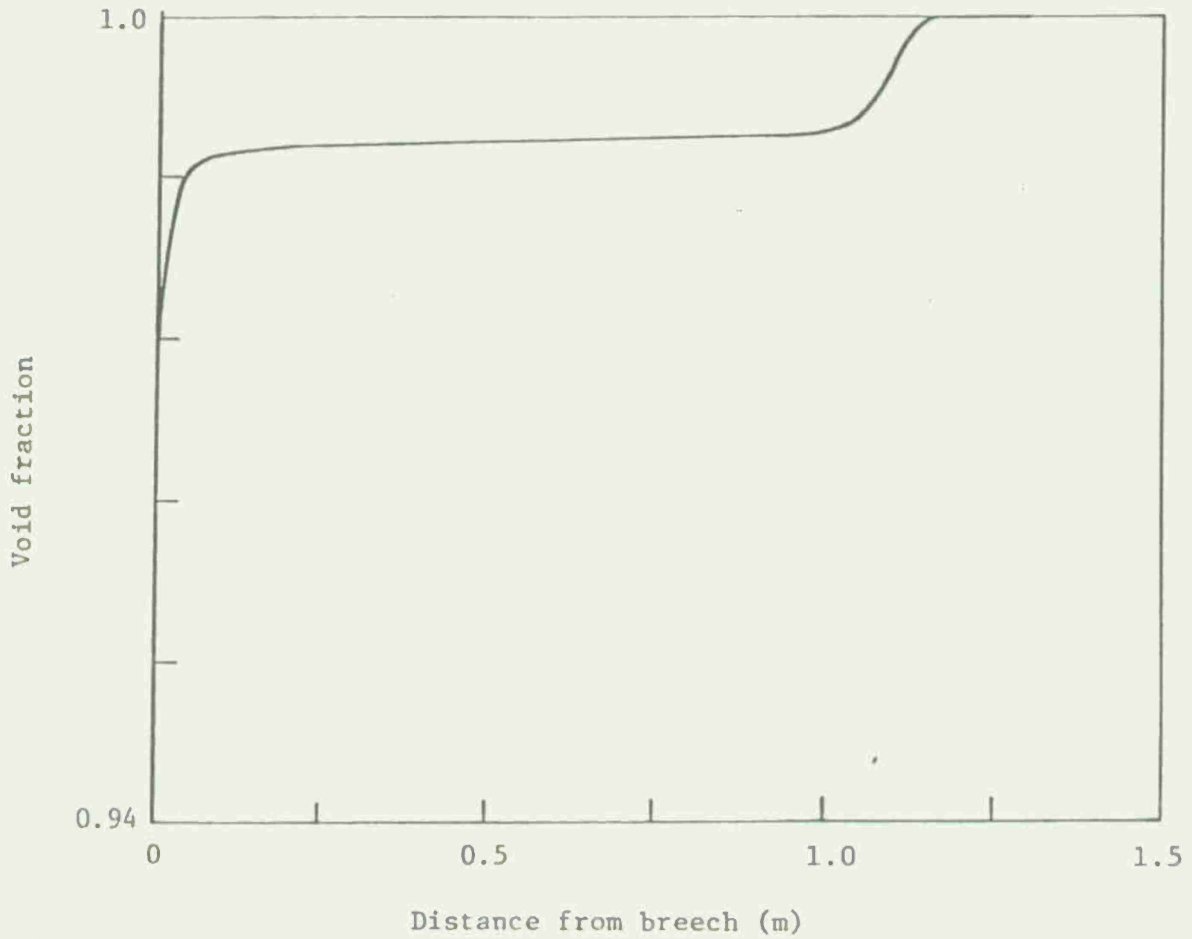

Figure 10 - Axial distribution of void fraction at tube centerline at muzzle exit time, t = 2.673 ms.

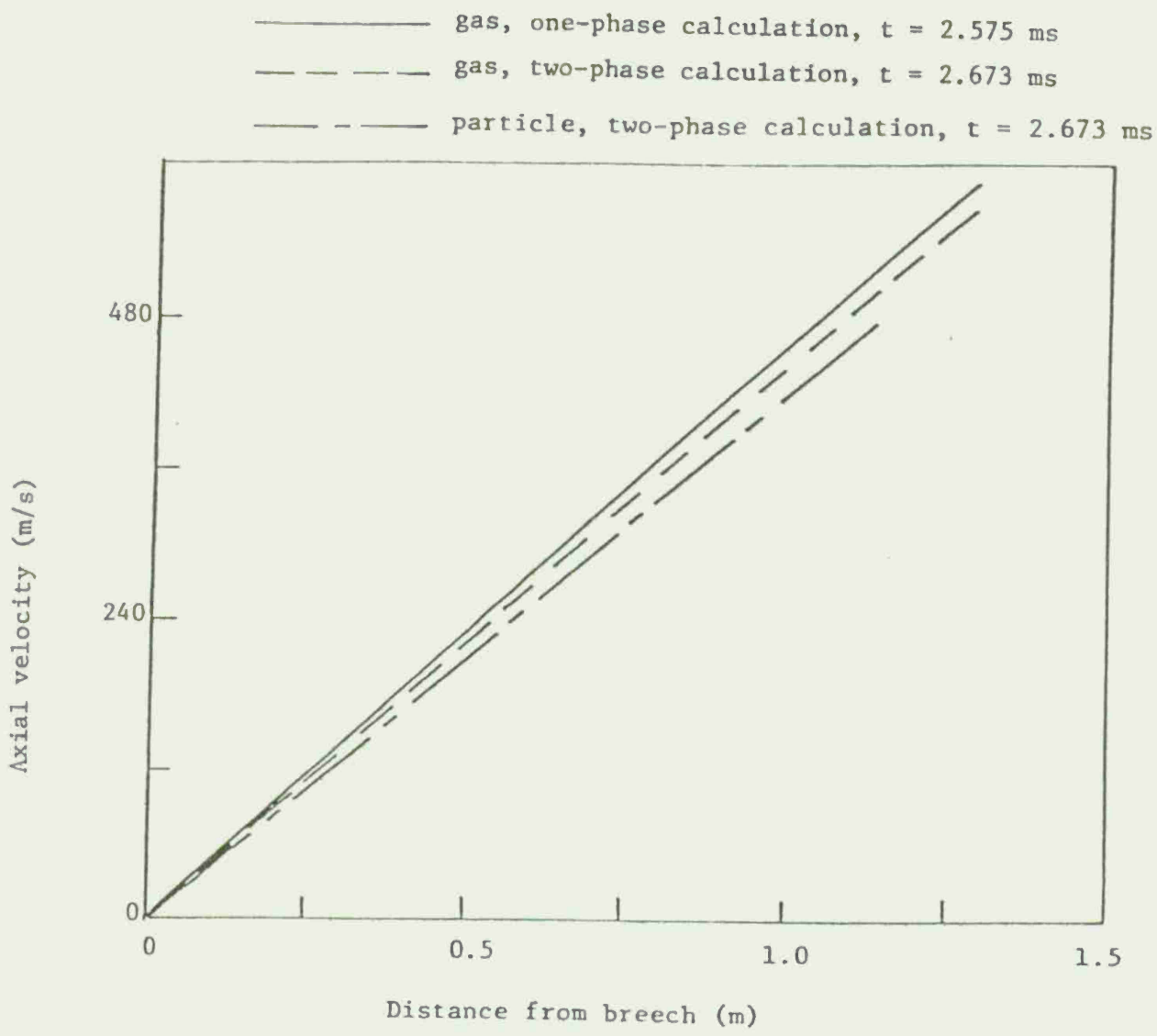

Figure 11 - Comparison of axial velocity distributions at tube centerline for one- and two-phase calculations at muzzle exit time.

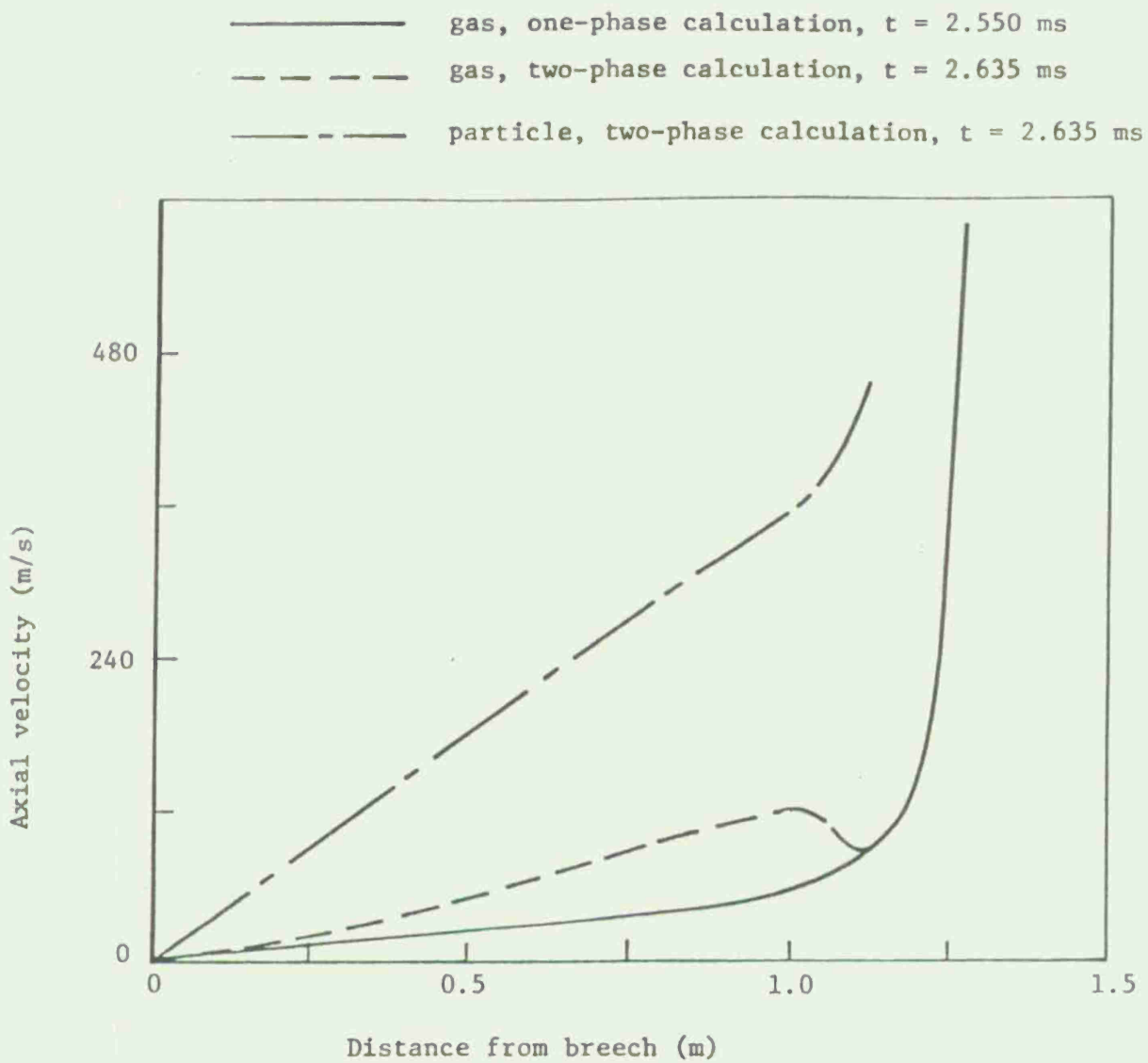

Figure 12 - Comparison of axial velocity distributions at r = 9.9924 mm for one- and two-phase calculations near muzzle exit time.

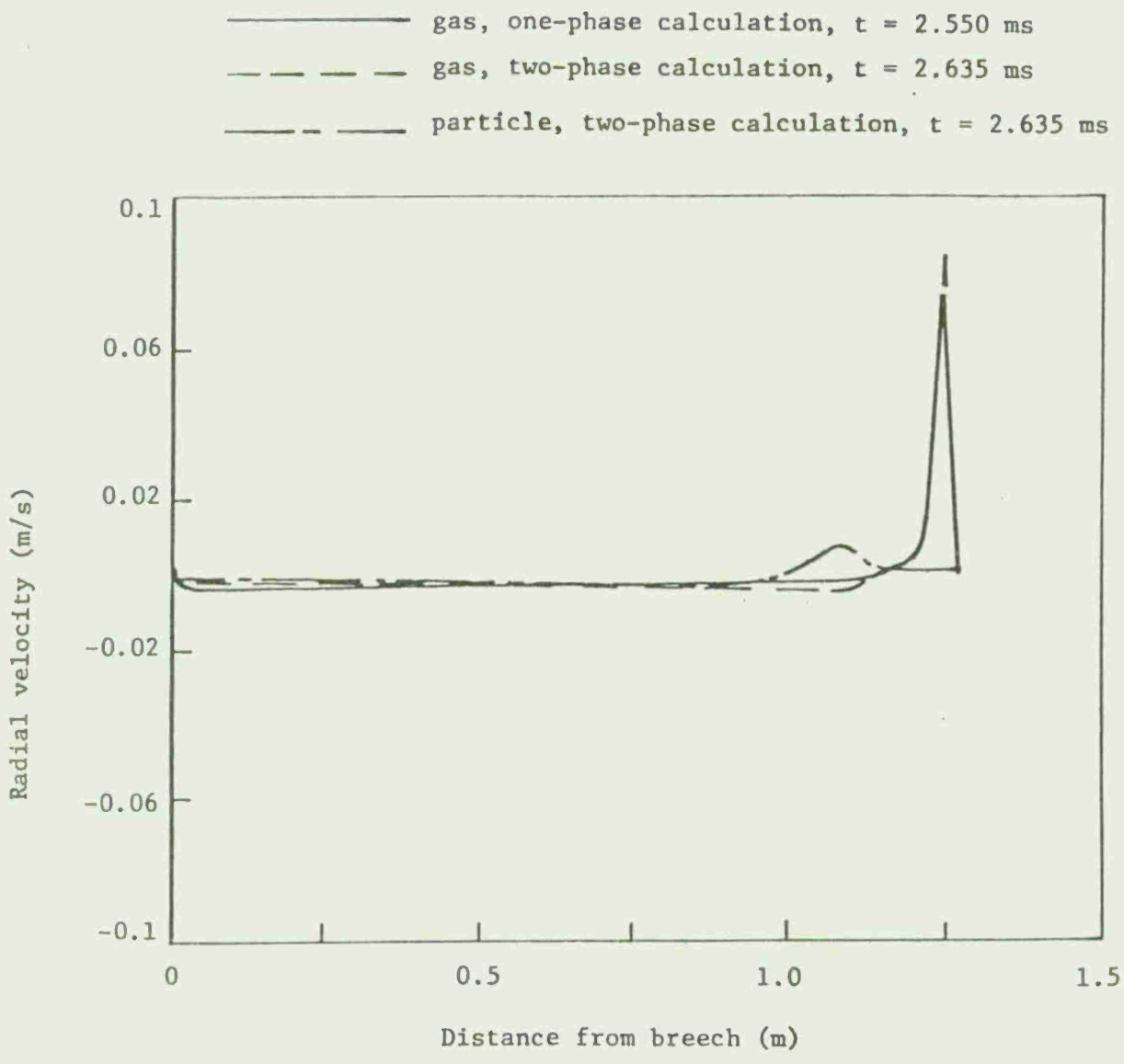

Figure 13 - Comparison of radial velocity distributions at r = 9.9924 mm for one- and two-phase calculations near muzzle exit time.

lower gas velocity in the two-phase results reflects the energy required to accelerate the solid particles. Radial direction distributions of pressure, density and temperature are shown in Figures 14, 15 and 16, respectively, while axial direction distributions are shown in Figures 17, 18 and 19, respectively. An abrupt change in pressure near the tube wall-projectile corner (Figure 17) is evident due to the discontinuous change in velocity from the projectile base to the tube wall. The density and temperature variation near the projectile base are known to be inaccurate with a uniform axial mesh (Reference 16). One-phase calculations performed by Reference 16 with a refined axial mesh near the projectile base did not exhibit either the increase in temperature or decrease in density as the projectile is approached near the tube wall. As mentioned previously, this problem area must be addressed carefully to improve computed results in the corner region.

In the present calculations, total system mass and energy are computed periodically as a check on the spatial and temporal accuracy of the finite difference computations. In the one-phase case, the total energy of the system consists of gas internal energy, gas kinetic energy and projectile kinetic energy. For the one-phase results, the final mass and energy of the system differed from starting values by -0.16% and -0.23%, respectively. In the two-phase case, total energy consists of gas internal energy, gas kinetic energy, particle internal energy (constant for thermally insulated particles), particle kinetic energy, and projectile kinetic energy. For the two-phase results, the final mass and energy of the system differed from starting values by 0.17% and -3.11%, respectively. The larger discrepancy in energy conservation in the two-phase calculation is believed to be associated with inadequate resolution of the interface between the pure gas zone and the gas-particle mixture near the projectile. Ultimately, an adaptive mesh transformation should be implemented to concentrate more grid points near such an interface in order to reduce local spatial truncation errors.

IV. CONCLUSIONS

The present two-phase, averaged Navier-Stokes analysis has been applied to the two-phase flow in a Lagrange gun. A consistently split, linearized, block implicit numerical procedure has been employed to solve the governing partial differential equations. This initial two-phase flow application has been restricted to laminar flow and adiabatic wall conditions; however, the ability of the computer code to solve the governing equations has been demonstrated.

It has been noted that the interphase correlations must be examined to include near wall effects, and the influence of particle-wall interaction must be determined. These areas will require more detailed experimental measurements than are presently available, and to this end

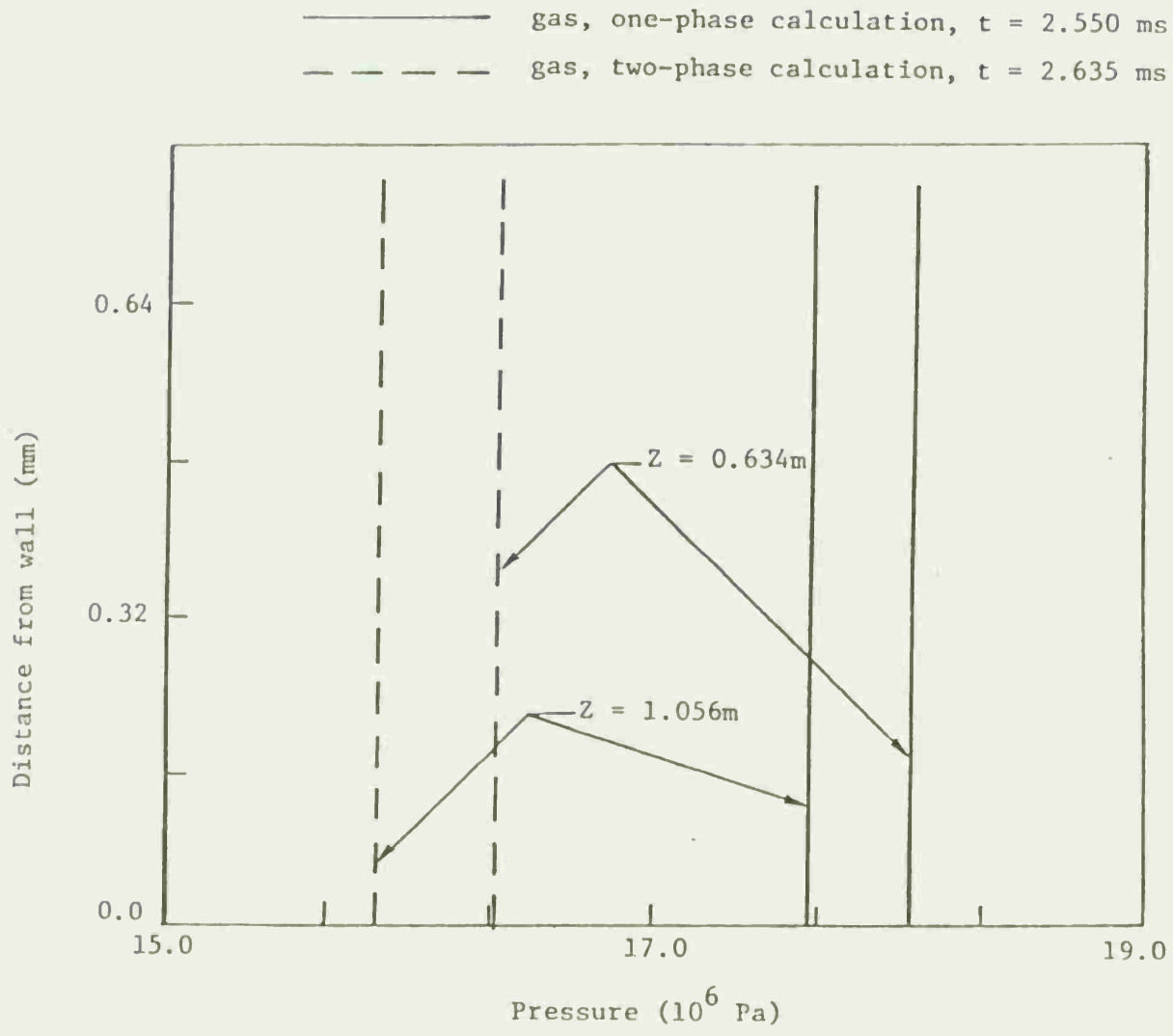

Figure 14 - Comparison of boundary layer pressure profiles for one- and two-phase calculations at two axial locations near muzzle exit time.

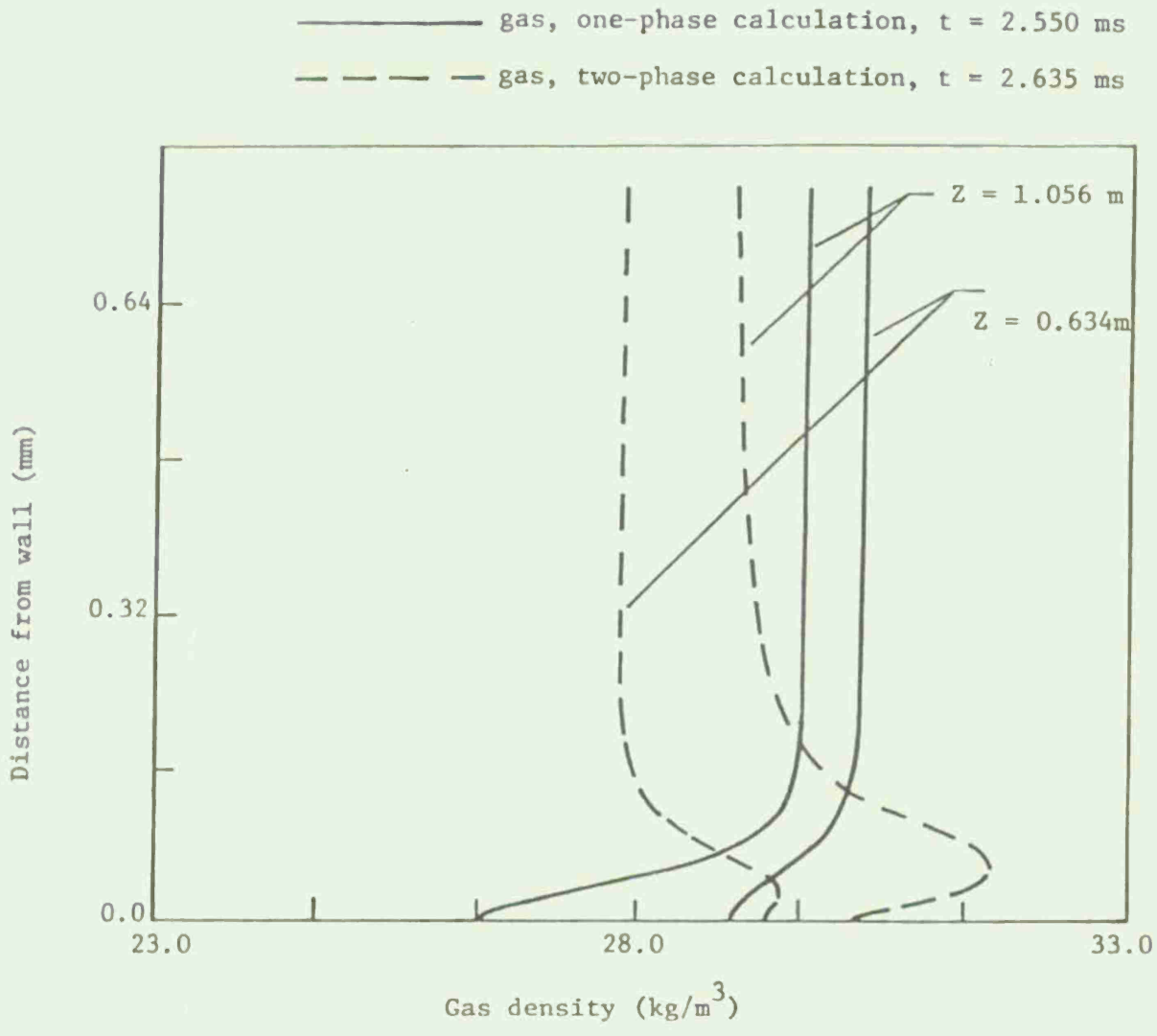

Figure 15 - Comparison of boundary layer density profiles for one- and two-phase calculations at two axial locations near muzzle exit time.

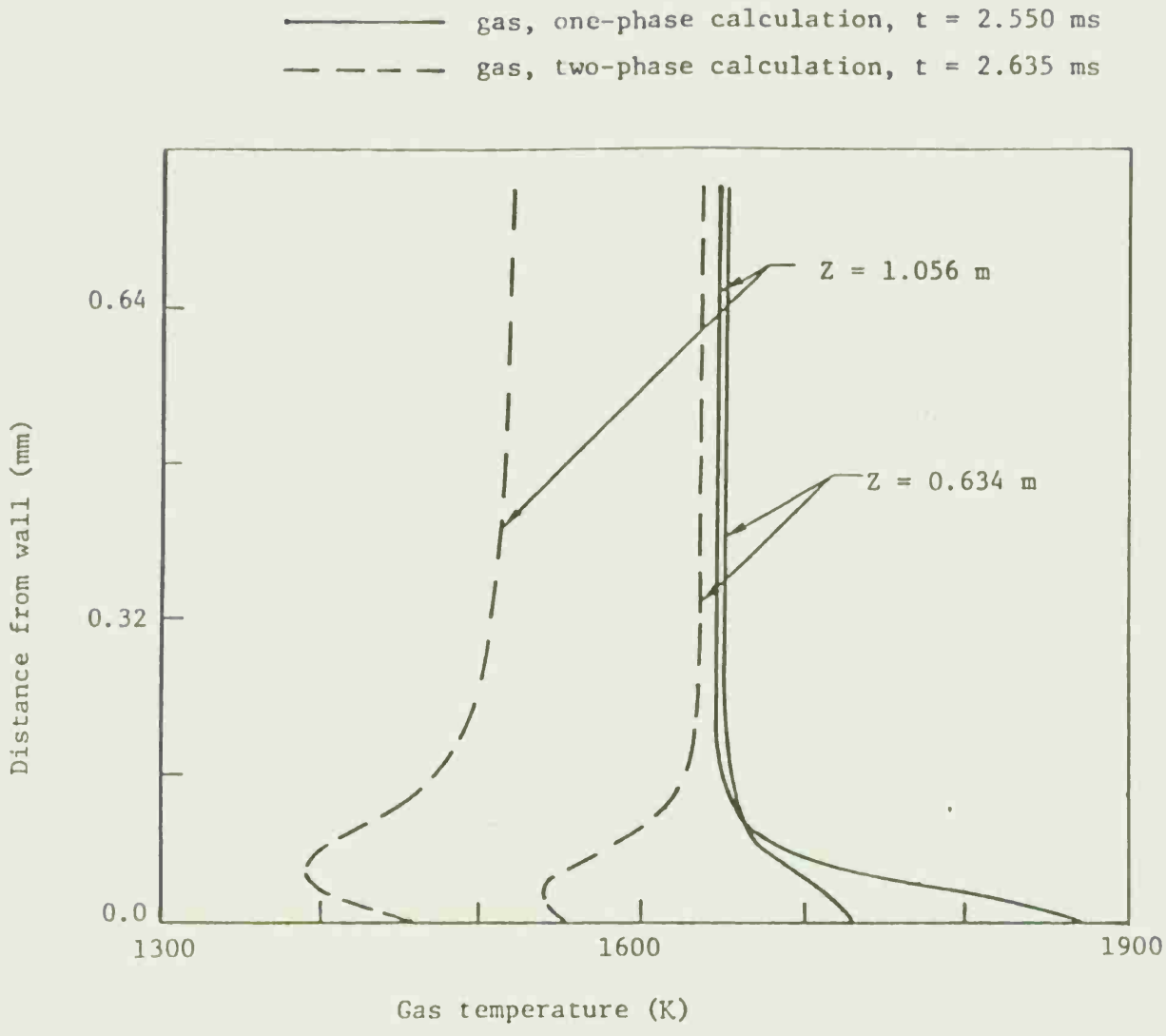

Figure 16 - Comparison of boundary layer temperature profiles for one- and two-phase calculations at two axial locations near muzzle exit time.

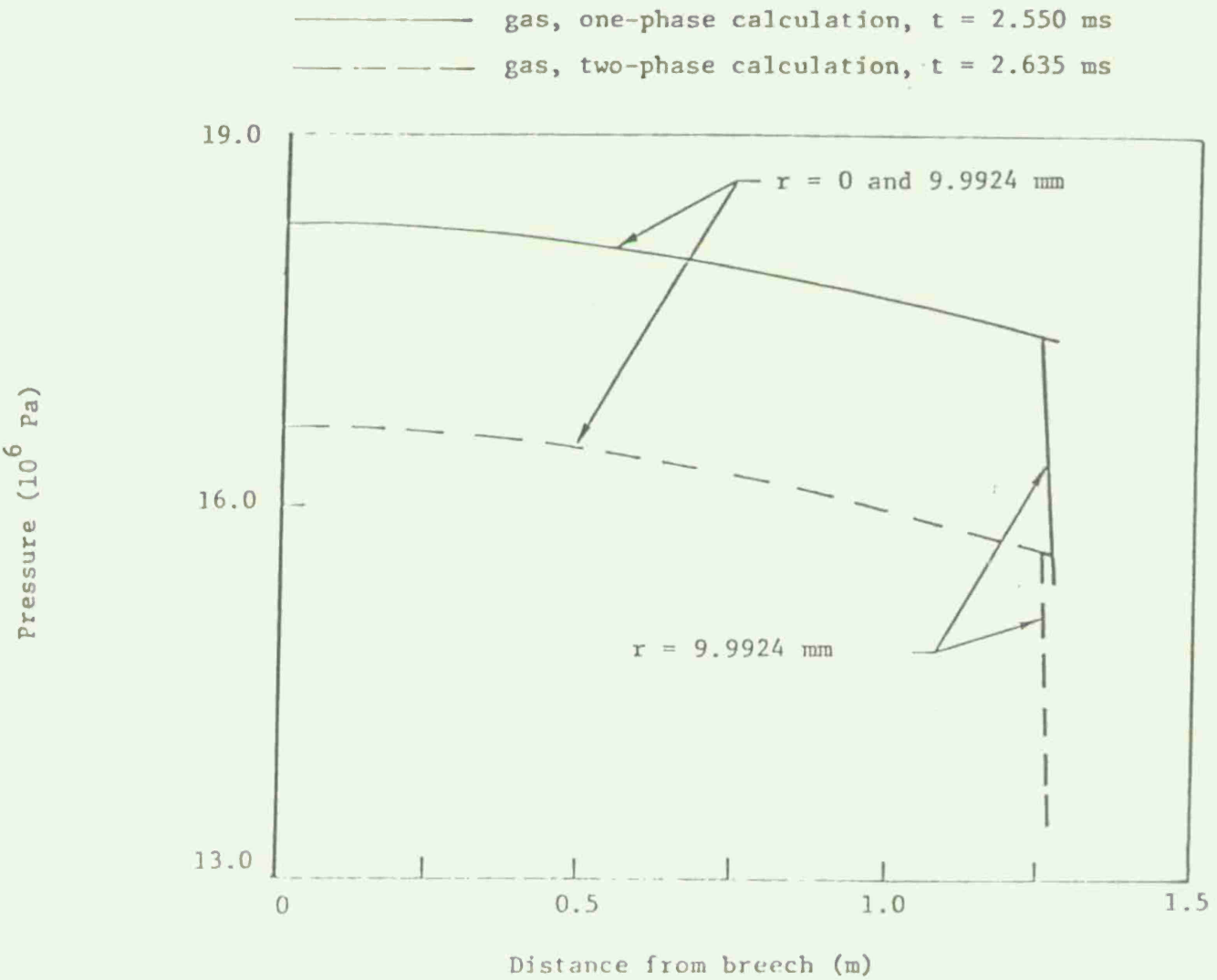

Figure 17 - Comparison of pressure distributions for one- and two-phase calculations at two radial locations near muzzle exit time.

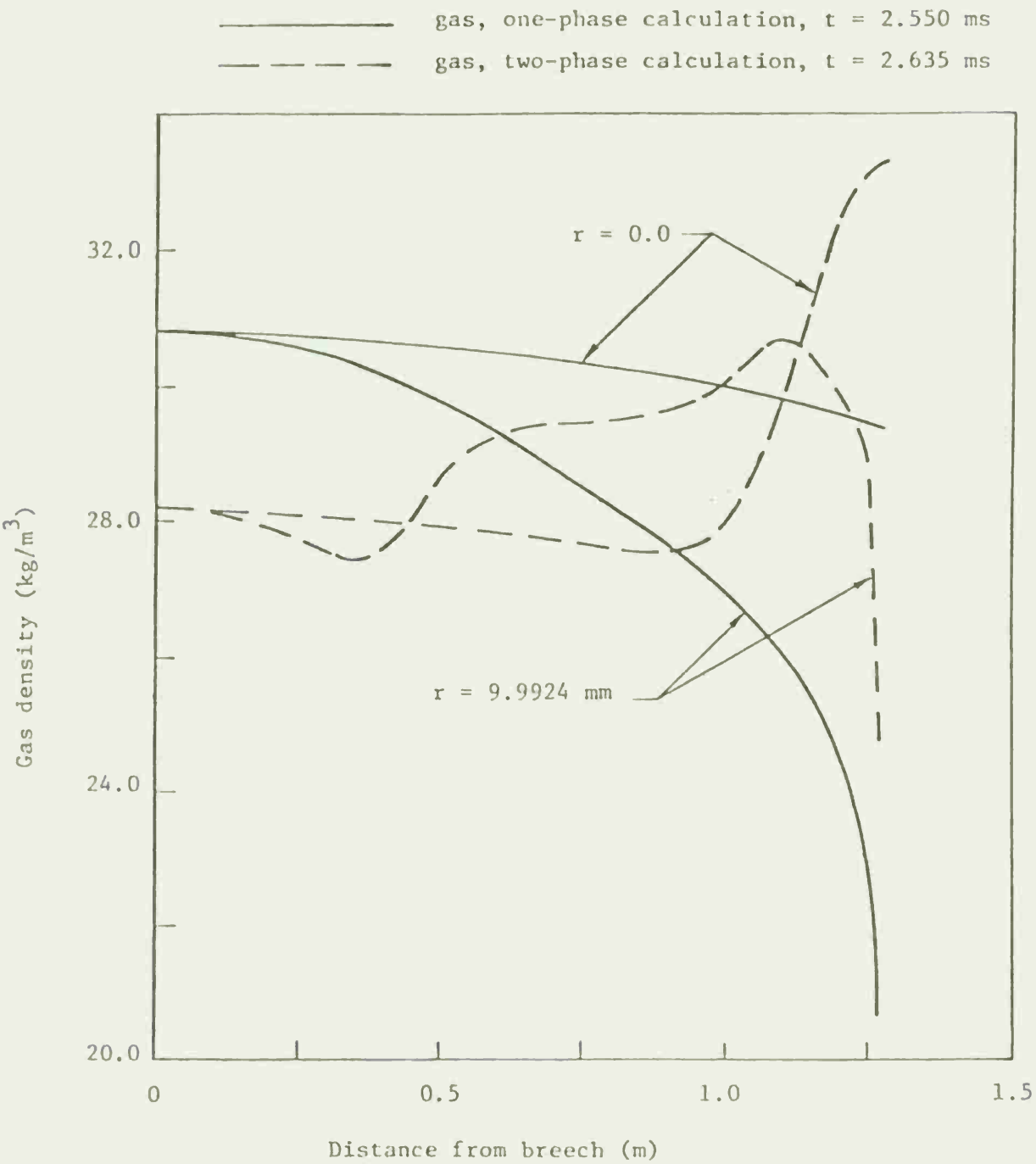

Figure 18 - Comparison of density distributions for one- and two-phase calculations at two radial locations near muzzle exit time.

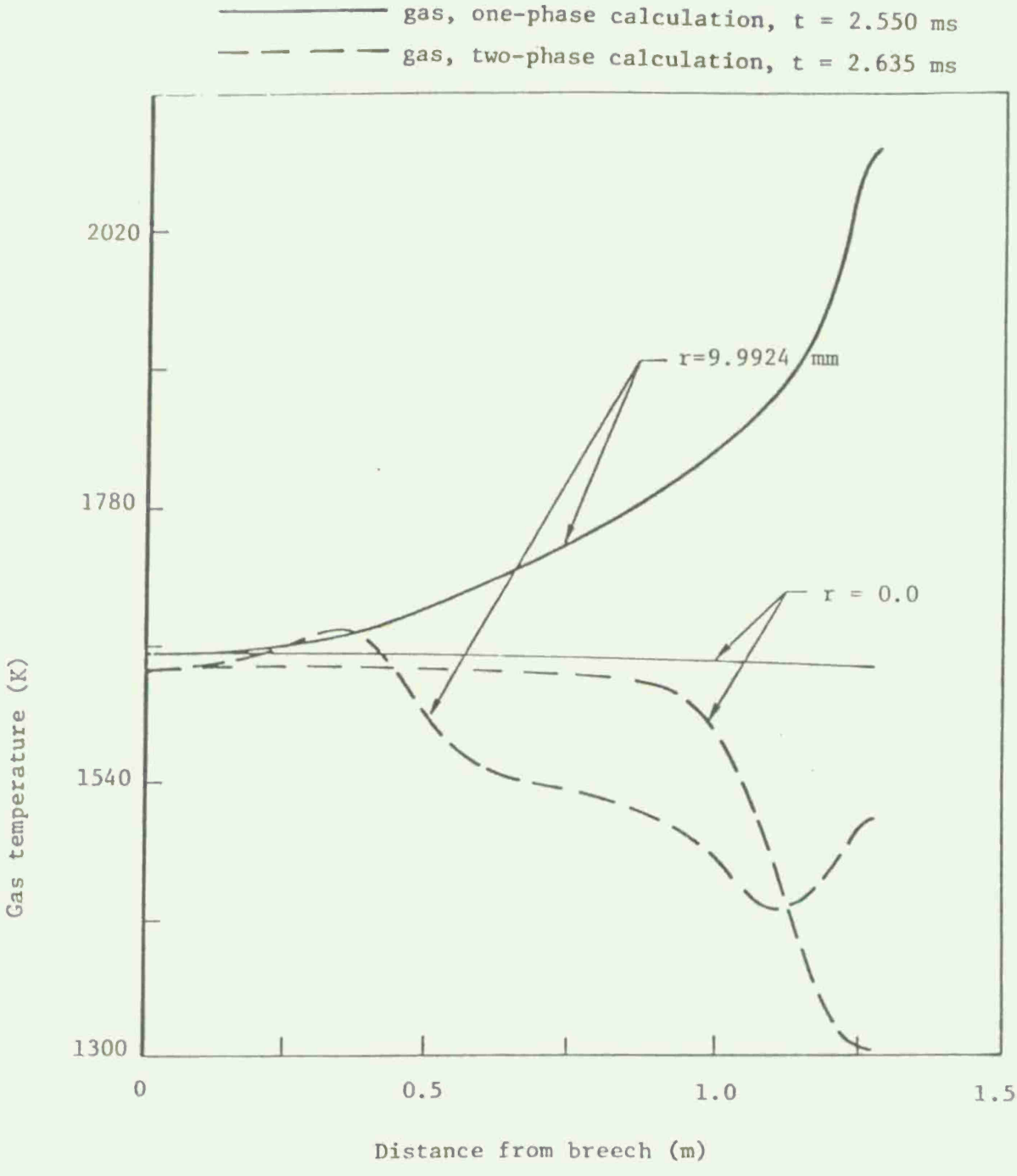

Figure 19 - Comparison of temperature distributions for one- and two-phase calculations at two radial locations near muzzle exit time.

benchmark experiments in a simulated ballistic environment have been designed by BRL personnel and J. Whitelaw of Imperial College. The resulting data will be used in future modeling efforts for both improvement of the interphase correlations and verification of turbulence models for two-phase flows in gun tubes.

REFERENCES

1. Gough, P.S. and Zwarts, F.J., "Modeling Heterogeneous Two-Phase Reacting Flow," AIAA Journal, Vol. 17, No. 1, pp. 17-25, 1979.

2. Kuo, K.K., Koo, J.H., Davis, T.R. and Coates, G.R., "Transient Combustion in Mobile Gas-Permeable Propellants," Acta Astronautica, Vol. 3, pp. 573-591, 1976.

3. Fisher, E.B., Graves, K.W. and Trippe, A.P., "Application of a Flame Spread Model to Design Problems in the 155 mm Propelling Charge,"12th JANNAF Combustion Meeting, CPIA Pub. 273, Vol. I, pp. 199-219, December 1975.

4. Krier, H., and Kokhale, S.S., "Modeling of Convective Mode Combustion Through Granulated Propellant to Predict Detonation Transition,"AIAA Journal, Vol. 16, No. 2, pp. 177-183, 1978.

5. Gough, P.S., "A Two-Dimensional Model of the Interior Ballistics of Bagged Artillery Charges," Paul Gough Associcates, Inc., Report PGA-TR-81-1, Portsmouth, NH, 1981.

6. Gibeling, H. J., Buggeln R.C. and McDonald, H., "Development of a Two-Dimensional Implicit Interior Ballistics Code," US Army ARRADCOM/Ballistic Research Laboratory, Contract Report ARBRL-CR-00411, Aberdeen Proving Ground, MD, January 1980 (AD A084092).

7. Gibeling, H.J. and McDonald, H., "Development of a Two-Dimensional Implicit Interior Ballistics Code," US Army ARRADCOM/Ballistic Research Laboratory, Contractor Report ARBRL-CR-00451, Aberdeen Proving Ground, MD, March 1981 (AD A100276).

8. Schmitt, J.A., Banks, N.E., Zoltani, C.K., Gibeling, H.J. and Mann, T.L., "Two-Phase Viscous Flow Modeling of Interior Ballistics, Algorithm and Numerical Predictions for an Idealized Lagrange Gun," Proceedings of the ASME Symposium on Computers in Flow Predictions and Fluid Dynamic Experiments, Edited by K.N. Ghia, T.J. Mueller and B.R. Patel, pp. 181-190, 1981.

9. Gough, P.S., "Derivation of Balance Equations for Heterogeneous Two-Phase Flow by Formal Averaging," ARO Workshop on Multiphase Flows, USA Ballistic Research Laboratory, pp. 71-80, February 1978.

10. Gough, P.S., "The Flow of a Compressible Gas Through an Aggregate of Mobile, Reacting Particles," Ph.D Thesis, Department of Mechanical Engineering, McGill University, Montreal, 1974.

11. Ishii, M., Thermo-Fluid Dynamic Theory of Two-Phase Flow, Eyrolles, Paris, 1975.

12. Briley, W.R. and McDonald, H., "Solution of the Multidimensional Compressible Navier-Stokes Equations by a Generalized Implicit Method," Journal of Computational Physics, Vol. 24, No. 4, pp. 372-397, 1977.

13. Briley, W.R. and McDonald, H., "On the Structure and Use of Linearized Block Implicit Schemes," Journal of Computational Physics, Vol. 34, No. 1, pp. 54-73, 1980.

14. Love, E.H. and Pidduck, F.B., "Lagrange's Ballistic Problem," Phil. Trans. Roy. Soc., Vol. 222, pp. 167-226, 1921-22.

15. Heiser, R. and Hensel, D., "Berechnung der Gasströmung in einem Waffenrohr mit Hilfe des Zweidimensionalen AMI-Modells," E1/81, Ernest-Mach-Institut, Abteilung fur Ballistik, Weil am Rhein, West Germany, January 1981.

16. Schmitt, J.A. and Mann, T.L., "Calculation of the Compressible Flow in the Lagrange Gun by the Interior Ballistics Algorithm Alpha," Proceedings of the DEA-G-1060 Meeting, Eglin Air Force Base, October 1980.

A-1. Gough, P.S., "Numerical Analysis of a Two-Phase Flow with Explicit Internal Boundaries," IHCR 77-5, Naval Ordnance Station, Indian Head, MD, April 1977.

A-2. Thomas, P.D. and Lombard, C.K., "Geometric Conservation Law and Its Application to Flow Computations on Moving Grids," AIAA Journal, Vol. 17, No. 10, p. 1030, 1979.

A-3. Ergun, S., "Fluid Flow Through Packed Columns," Chem. Eng. Progr., Vol. 48, p. 89, 1952.

A-4. Celmiņš, A., Private communication, US Army Ballistic Research Laboratory, 1982.

APPENDIX A

GOVERNING EQUATIONS

A. Governing Equations

The averaged time-dependent governing partial differential equations for the turbulent, two-phase flow in a gun tube were presented in References 6 and 7. The equations are summarized here in dimensional form with corrections where required.

The gas and solid phase continuity equations are, respectively,

$$\frac{\partial(\alpha\rho)}{\partial t} + \nabla\cdot(\alpha\rho\vec{U}) = \Gamma \qquad \text{(A-1)}$$

$$\frac{\partial(1-\alpha)\rho_p}{\partial t} + \nabla\cdot\left[(1-\alpha)\rho_p\vec{U}_p\right] = -\Gamma \qquad \text{(A-2)}$$

where the void fraction (or porosity) α is the ratio of volume occupied by the gas phase to the total volume. The averaged densities and velocities of the gas and solid phases are ρ, $\vec{U}$, ρ_p, $\vec{U}_p$, respectively. The interphase mass transfer rate Γ, Eq. (A-12), is due to propellant burning. The gas and solid phase momentum equations are, respectively,

$$\frac{\partial(\alpha\rho\vec{U})}{\partial t} + \nabla\cdot(\alpha\rho\vec{U}\vec{U}) = -\alpha\nabla p + \nabla\cdot\left[\alpha\left(\bar{\bar{\pi}} + \bar{\bar{\pi}}^T\right)\right] \qquad \text{(A-3)}$$

$$-(1-\alpha)\frac{S_p}{V_p}\langle\vec{F}\rangle + \vec{U}_p\Gamma$$

$$\frac{\partial\left[(1-\alpha)\rho_p\vec{U}_p\right]}{\partial t} + \nabla\cdot\left[(1-\alpha)\rho_p\vec{U}_p\vec{U}_p\right] = -(1-\alpha)\nabla p \qquad \text{(A-4)}$$

$$+\nabla\left[(1-\alpha)R_p\right] + (1-\alpha)\frac{S_p}{V_p}\langle\vec{F}\rangle - \vec{U}_p\Gamma$$

where p is the averaged pressure. The tensors $\bar{\bar{\pi}}$ and $\bar{\bar{\pi}}^T$, Equations (A-16) and (A-19), are the averaged molecular and turbulent stress tensors in the gas phase, respectively. The constitutive relations for the propellant grain surface area S_p, volume V_p, the interphase drag $\langle\vec{F}\rangle$, and the isotropic intergranular stress R_p are given by Equations (A-13), (A-14), (A-22), and (A-25), respectively.

The gas phase energy equation is

$$\frac{\partial(\alpha\rho h)}{\partial t} + \nabla\cdot(\alpha\rho\vec{U}h) = -\nabla\cdot\left[\alpha(\vec{q}+\vec{q}^T)\right] + \frac{D}{Dt}(\alpha p) + \alpha\bar{\Phi} + \alpha\Phi^T + \Lambda \tag{A-5}$$

where h is the averaged static enthalpy of the gas. The mean flow energy dissipation Φ, the turbulent energy dissipation Φ^T, the interphase energy transfer Λ, and the molecular and turbulent heat flux vectors $\vec{q}$ and $\vec{q}^T$ are given by Equations (A-26), (A-27), (A-28), (A-34) and (A-35), respectively. Also, the symbol D/Dt denotes the substantial derivative, i.e.,

$$\frac{D}{Dt} = \frac{\partial}{\partial t} + \vec{U}\cdot\nabla \tag{A-6}$$

The Nobel-Abel equation of state, Equation (A-37), relates the gas pressure to the density and temperature. The turbulence kinetic energy equation is given by

$$\frac{\partial(\alpha\rho k)}{\partial t} + \nabla\cdot(\alpha\rho\vec{U}k) = \nabla\cdot\left(\alpha\frac{\mu_T}{\sigma_k}\nabla k\right) + \alpha\left\{\mu_T\left[2\bar{\bar{D}}:\bar{\bar{D}} - \frac{2}{3}(\nabla\cdot\vec{U})^2\right] - \frac{2}{3}\rho k\nabla\cdot\vec{U} - \rho\epsilon\right\} + S_k \tag{A-7}$$

where $\sigma_k = 1.0$ is used, and the interphase turbulence production, S_k, is neglected at present. The rate of strain tensor $\bar{\bar{D}}$ and the turbulent viscosity μ_T are given by Equations (A-17) and (A-20), respectively.

Exclusion of gas phase chemical reactions from the present analysis eliminates the need for gas phase and gasified propellant species mass fraction equations. However, in order to consider several types of propellants in the system, transport equations for the reciprocal gas mixture molecular weight parameter $Z = R_u/W_m$ and the specific heat at constant pressure must be solved; these are

$$\frac{\partial}{\partial t}(\alpha\rho Z) + \nabla\cdot(\alpha\rho\vec{U}Z) = \nabla\cdot\left[\alpha\Gamma_m\nabla Z\right] + Z_p\Gamma \qquad \text{(A-8)}$$

and

$$\frac{\partial(\alpha\rho c_p)}{\partial t} + \nabla\cdot(\alpha\rho\vec{U}c_p) = \nabla\cdot\left[\alpha\Gamma_m\nabla c_p\right] + (c_p)_p\Gamma \qquad \text{(A-9)}$$

where Z_p and $(c_p)_p$ are the reciprocal molecular weight parameter and specific heat of the propellant, respectively, and $\Gamma_m = \mu_{eff}/Sc_{eff} = \mu_{eff} = \mu + \mu_T$, and the effective Schmidt number is taken as $Sc_{eff} = 0.9$.

At present, the propellant grains are assumed to be spherical. The surface temperature of these particles is desired to determine ignition, the rate of heat transfer between the gas and solid phases, and possibly the propellant burning rate. By assuming that the penetration depth of the thermal wave into the propellant grains is small compared to the grain dimensions, it is permissible to use a one-dimensional approximation to obtain the propellant surface temperature. Following the motion of a given particle, the heat conduction equation for the propellant temperature T_p is

$$\left(\frac{dT_p}{dt}\right)_{\tilde{r}} = \frac{d_p}{\tilde{r}^2}\frac{\partial}{\partial\tilde{r}}\left(\tilde{r}^2\frac{\partial T_p}{\partial\tilde{r}}\right) \qquad \text{(A-10)}$$

where $T_p = T_p(r;\vec{x},t)$ is the phase-averaged temperature within a representative particle, r is the radial location within the spherical particle, d_p is the thermal diffusivity of the particles, and $(d/dt)_r$ denotes the Lagrangian time derivative at constant r within the particle. The relevant boundary condition for Equation (A-10) is a specified surface heat flux, Equation (A-41), which is determined using the interphase heat transfer relation, Equation (A-29), and a heat feedback relation, Equation (A-42), identified by Gough.[A-1] The actual

A-1. P.S. Gough, "Numerical Analysis of a Two-Phase Flow with Explicit Internal Boundaries," IHCR 77-5, Naval Ordnance Station, Indian Head, MD, April 1977.

burning is modeled as a regression of the propellant surface with a resulting deposition of mass, momentum and energy into the gas phase. The equation for average particle radius, r_p, including turbulent diffusion is

$$\frac{\partial\left[(1-\alpha)\rho_p r_p\right]}{\partial t} + \nabla\cdot\left[(1-\alpha)\rho_p \vec{U}_p r_p\right]$$

$$= \nabla\cdot\left[(1-\alpha)\Gamma_m \nabla r_p\right] - (1-\alpha)\rho_p\left(1 + r_p\frac{S_p}{V_p}\right)\langle\dot{d}\rangle \qquad \text{(A-11)}$$

where the surface regression rate $\langle\dot{d}\rangle$ is given by Equation (A-15). The relation for Γ, Equation (A-12), has been utilized in order to cast the particle radius equation into the above form.

The influence of the hot primer gas may be included in the procedure in two ways. The preferred approach is the application of mass flux and temperature boundary conditions near the tube centerline for a center core primer or at the breech end for a base primer. An alternative method would be the introduction of mass, momentum, and energy sources into the governing gas phase equations to represent the primer discharge.

The governing Equations (A-1) through (A- 9) and (A-11) are a system of general time-dependent nonlinear partial differential equations for two-phase flow. The applicability of these equations to a specific two-phase flow depends on the validity of both the averaging procedure and the constitutive relations, Equations (A-12) through (A-40), which complete the analysis. In order to solve these equations they must be written in a specific coordinate system. The governing equations in the ALPHA code were formulated in conservation form (Reference 7) by application of a nonorthogonal Jacobian transformation to the Equations (A-1) through (A- 9) and (A-11) written in cylindrical polar coordinates. A consistent technique for determination of the local time-dependent Jacobian determinant of the coordinate transformation was implemented in order to reduce geometrical errors in the computations, as suggested by Thomas and Lombard.[A-2] The resulting equations are solved for the following dependent variables: the radial, angular and axial components of gas velocity $\vec{U}$, the gas phase partial density $\alpha\rho$, the gas phase static enthalpy h, specific heat c_p, reciprocal molecular weight Z, and turbulence kinetic energy k. The solid phase dependent variables are the momentum flux components of $(1-\alpha)\rho_p\vec{U}_p$, the solid phase partial density $(1-\alpha)\rho_p$, and the particle radius parameter $(1-\alpha)\rho_p r_p$. The solid particle surface temperature is determined by solution of Equation (A-10) using boundary conditions Equations (A-41) and (A-42) after solution of the fully coupled system Equations (A-1) through (A- 9) and (A-11). Since the solution of Equations (A-1) through (A- 9) and (A-11) is an implicit one, the solid particle surface temperature must be treated explicitly

A-2. *P.D. Thomas and C.K. Lombard, "Geometric Conservation Law and Its Application to Flow Computations on Moving Grids," AIAA Journal, Vol. 17, No. 10, p. 1030, 1979.*

at present. This may result in a time step limitation to preserve transient accuracy; however, preliminary results indicate that this is not a severe restriction.

B. Constitutive Relations

Here we present the various constitutive relations required for closure of the two-phase flow Equations (A-1) through (A-11). The gas phase mass source due to propellant burning is

$$\Gamma = (1-\alpha)\frac{S_p \rho_p}{V_p} < \dot{d} > \qquad \text{(A-12)}$$

where the grain surface area, grain volume, and the steady state surface regression rate are given by

$$V_p = \frac{4}{3}\pi r_p^3 \qquad \text{(A-13)}$$

$$S_p = 4\pi r_p^2 \qquad \text{(A-14)}$$

$$< \dot{d} > = B_1 + B_2 p^n \qquad \text{(A-15)}$$

respectively. The constants B_1, B_2 and n are known for a given propellant. The gas molecular stress tensor for a Newtonian fluid is

$$\bar{\bar{\pi}} = 2\mu \bar{\bar{D}} - \left(\frac{2}{3}\mu - K_B\right)\nabla \cdot \vec{U}\,\bar{\bar{I}} \qquad \text{(A-16)}$$

where μ is the molecular viscosity, K_B is the bulk viscosity, and $\bar{\bar{I}}$ is the identity tensor. The rate of strain tensor is

$$\bar{\bar{D}} \equiv \frac{1}{2}\left[(\nabla \vec{U}) + (\nabla \vec{U})^{\text{TRANSPOSE}}\right] \qquad \text{(A-17)}$$

and the molecular viscosity is determined from Sutherland's law

$$\frac{\mu}{\mu_o} = \left(\frac{T}{T_o}\right)^{3/2} \frac{T_o + S_1}{T + S_1} \qquad \text{(A-18)}$$

where S_1 = 110 K, T_o = 300 K, and $\mu_o = 1.8463 \cdot 10^{-5}$ Pa-s. The bulk viscosity K_B is assumed to be zero. The turbulent stress tensor is modeled using an isotropic eddy viscosity formulation,

$$\bar{\bar{\pi}}^T = -\rho \overline{\vec{u}'\vec{u}'} = 2\mu_T \bar{\bar{D}} - \frac{2}{3}(\mu_T \nabla \cdot \vec{U} + \rho k)\bar{\bar{I}} \qquad \text{(A-19)}$$

$$\mu_T = C_\mu \frac{\rho k^2}{\epsilon} \qquad \text{(A-20)}$$

$$\epsilon = C_\mu^{3/4} \frac{k^{3/2}}{\ell} \qquad \text{(A-21)}$$

where the mixing length, ℓ, is specified algebraically and C_μ is a function of the turbulence Reynolds number, $R_T = \mu_T/\mu$.

The interphase drag relation $\langle \vec{F} \rangle$ is determined by a combination of Ergun's relation[A-3] for a packed bed of spheres and a fit to the drag coefficient data for isolated spheres.[A-4]

$$\langle \bar{F} \rangle = \begin{cases} \bar{F}_{REYN} & \text{for } \alpha \geq 0.9 \\ 4 \cdot \left[(\alpha - 0.65)\bar{F}_{REYN} + (0.9 - \alpha)\bar{F}_{ERGUN} \right] & \text{for } 0.65 < \alpha < 0.9 \\ \bar{F}_{ERGUN} & \text{for } \alpha < 0.65 \end{cases} \qquad \text{(A-22)}$$

$$\bar{F}_{ERGUN} = \frac{\rho \bar{U}_R}{6\alpha^2} \left[150(1-\alpha)\frac{\mu}{\rho 2 r_p} + 1.75 |\bar{U}_R| \right] \qquad \text{(A-23)}$$

A-3. S. Ergun, "Fluid Flow Through Packed Columns," Chem. Eng. Progr., Vol. 48, p. 89, 1952.

A-4. A. Celmiņš, Private communication, US Army Ballistic Research Laboratory, 1982.

$$\bar{F}_{REYN} = \frac{\rho \bar{U}_R}{4} \left[12 \frac{\mu}{\rho 2 r_p} + 0.2 |\bar{U}_R| \right] \qquad \text{(A-24)}$$

where $\vec{U}_R = \vec{U} - \vec{U}_p$.

The intergranular stress relation R_p which is independent of the loading history is given by

$$R_p = \begin{cases} -\rho_p a_p^2 \dfrac{\alpha_c - \alpha}{(1-\alpha)} \dfrac{\alpha_c}{\alpha} & \text{if} \quad \alpha \le \alpha_c \\ 0 & \text{if} \quad \alpha > \alpha_c \end{cases} \qquad \text{(A-25)}$$

where a_p is the speed of sound in the solid phase which is specified for a given propellant, and α_c is a critical porosity above which there is no direct contact between particles. The mean flow dissipation function Φ is given by

$$\Phi = 2\mu \bar{\bar{D}} : \bar{\bar{D}} - \left(\frac{2}{3} \mu - K_B \right) (\nabla \cdot \vec{U})^2 \qquad \text{(A-26)}$$

and the turbulence energy dissipation is approximated by

$$\Phi^T = 2\mu_T \bar{\bar{D}} : \bar{\bar{D}} - \frac{2}{3} \mu_T (\nabla \cdot \vec{U})^2 \qquad \text{(A-27)}$$

The interfacial energy transfer Λ is defined by

$$\begin{aligned} \Lambda = & -p(\vec{U} - \vec{U}_p) \cdot \nabla \alpha \\ & + (1-\alpha) \frac{S_p}{V_p} (\vec{U} - \vec{U}_p) \cdot \langle \vec{F} \rangle + \vec{q} \cdot \nabla \alpha \\ & - (1-\alpha) \frac{S_p}{V_p} \langle q \rangle + \Gamma \left[h_{comb} + \frac{1}{2} (\vec{U} - \vec{U}_p) \cdot (\vec{U} - \vec{U}_p) \right] \end{aligned} \qquad \text{(A-28)}$$

where h_{comb} is the energy released per unit mass due to combustion of the propellant. The interphase heat transfer $\langle q \rangle$ is given by

$$\langle q \rangle = h_t (T - T_{ps}) \tag{A-29}$$

where the total heat transfer coefficient h_t is

$$h_t = \frac{\kappa}{2r_p} Nu_p + \epsilon_p \sigma (\bar{\bar{T}} + \bar{\bar{T}}_{ps})(\bar{\bar{T}}^2 + \bar{\bar{T}}_{ps}^2) \tag{A-30}$$

where ϵ_p is the propellant emissivity, σ is the Stefan-Boltzmann constant, and the propellant surface temperature is determined from the solution of Equation (A-10). The Nusselt number correlation used is

$$Nu_p = 2.0 + 0.4 Re_p^{2/3} Pr^{1/3} \tag{A-31}$$

where the Prandtl number is $Pr = \mu c_p/\kappa$ and the particle Reynolds number is defined as

$$Re_p = \frac{2r_p \rho |\vec{U}_R|}{\mu} \tag{A-32}$$

The thermal conductivity κ is determined from Sutherland's law,

$$\frac{\kappa}{\kappa_0} = \left(\frac{T}{T_0}\right)^{3/2} \frac{T_0 + S_2}{T + S_2} \tag{A-33}$$

where $S_2 = 194$ K, $T_0 = 300$ K, and $\kappa_0 = 2.6273$ W/(m-K). The mean and turbulent heat flux vectors may be written as

$$\vec{q} = -\kappa \left[\nabla T - \frac{\nabla a}{a} (T_i - T) \right] \tag{A-34}$$

and

$$\vec{q}^{T} = -\kappa^{T}\left[\nabla T - \frac{\nabla a}{a}\left(T_i - T\right)\right] \tag{A-35}$$

where the turbulent thermal conductivity is defined from

$$\kappa^{T} = \frac{c_p \mu_{eff}}{Pr_{eff}} - \kappa \tag{A-36}$$

with $Pr_{eff} = 0.9$. The mean temperature at the interface between the phases, T_i, is assumed to be the average $T_i = 0.5\ (T + T_{ps})$.

The Nobel-Abel equation of state for the gas is

$$p(1 - \rho\eta) = \frac{\rho R_u T}{W_m} \equiv \rho Z T \tag{A-37}$$

where R_u is the universal gas constant, W_m is the gas molecular weight and η is the covolume factor which provides a correction to the perfect gas equation of state for large density. Other required thermodynamic properties are

$$c_p \equiv \left.\frac{\partial h}{\partial T}\right|_p = c_v + Z \tag{A-38}$$

and

$$\gamma = \frac{c_p}{c_v} \tag{A-39}$$

$$h = c_p T + \eta p \tag{A-40}$$

The required boundary condition for Equation (A-10) at the propellant grain surface is the surface heat flux relation,

$$k_p \frac{\partial T_p}{\partial \tilde{r}} (\tilde{r} = r_p, 1) = \langle q \rangle + k_p \phi (\langle \dot{d} \rangle, p) \qquad \text{(A-41)}$$

where $\langle q \rangle$ is given by Equation (A-29), k_p is the particle thermal conductivity, and ϕ is the heat feedback from the flame identified by Gough (Reference 17) as

$$\phi = \frac{\langle \dot{d} \rangle}{d_p} (T_{ps} - T_{po}) \qquad \text{(A-42)}$$

where d_p is the thermal diffusivity of the particles and T_{po} is taken as the temperature at the center of the particle. Following Reference 17, the heat feedback is utilized only for the transient combustion analysis and is excluded when steady state combustion is assumed.

DISTRIBUTION LIST

No. of Copies	Organization
12	Commander Defense Technical Info Center ATTN: DTIC-DDA Cameron Station Alexandria, VA 22314
2	HQDA(DAMA-CSM-CS, LTC Townsend, COL Zimmerman) Washington, DC 20310
1	Commander USA Materiel Development and Readiness Command ATTN: DRCDMD-ST 5001 Eisenhower Avenue Alexandria, VA 22333
3	Commander Armament R&D Ctr USA AMCCOM ATTN: DRSMC-CG(D) Dover, NJ 07801
6	Commander Armament R&D Ctr, USA AMCCOM ATTN: DRSMC-TSS(D) DRSMC-LC(D) J.T. Frasier DRSMC-LCA-M(D), F. Saxe Dover, NJ 07801
6	Commander Armament R&D Ctr, USA AMCCOM ATTN: DRSMC-LCU(D) DRSMC-LCU-E(D) Dover, NJ 07801
5	Commander Armament R&D Ctr, USA AMCCOM ATTN: DRSMC-LCU-EP(D) DRSMC-LCU-S(D) DRSMC-TDS (D) DRSMC-TD(D) DRSMC-TDC(D) Dover, NJ 07801
1	Commander USA Armament, Mun & Chem Cmd ATTN: DRSMC-LEP-L(R) Rock Island, IL 61299
1	Director Armament R&D Ctr, USA AMCCOM Benet Weapons Laboratory ATTN: DRSMC-LCB-TL(D) Watervliet, NY 12189
1	Commander US Army Aviation Research and Development Command ATTN: DRDAV-E 4300 Goodfellow Blvd St. Louis, MO 63120
1	Director USA Air Mobility R&D Lab Ames Research Center Moffett Field, CA 94035
1	Commander US Army Communications Rsch and Development Command ATTN: DRSEL-ATDD Fort Monmouth, NJ 07703
1	Commander US Army Electronics Research and Development Command Technical Support Activity ATTN: DELSD-L Fort Monmouth, NJ 07703
1	Commander US Army Missile Command ATTN: DRSMI-R Redstone Arsenal, AL 35898
1	Commander US Army Missile Command ATTN: DRSMI-YDL Redstone Arsenal, AL 35898

DISTRIBUTION LIST

No. of Copies	Organization
1	Commander US Army Tank Automotive Command ATTN: DRSTA-TSL Warren, MI 48090
6	Project Manager Cannon Artillery Weapons System ATTN: DRCPM-CAWS(3 cys) DRCPM-CAWS-GP DRCPM-CAWS-WP DRCPM-SA Dover, NJ 07801
3	Project Manager M110E2 Weapons Systems ATTN: DRCPM-M110E2-TM, S. Smith R. Newlon B. Walters Rock Island, IL 61299
2	Commander USA Research Office P.O. Box 12211 ATTN: J. Chandra E. Singleton Research Triangle Park NC 27709
1	Director US Army TRADOC Systems Analysis Activity ATTN: ATAA-SL White Sands Missile Range NM 88022
1	Commandant US Army Field Artillery School ATTN: APSF-CD-W, LT Monigal Fort Sill, OK 73503
2	Commander Naval Surface Weapons Center ATTN: J. East Tech Lib Dahlgren, VA 22448
1	Commander Naval Weapons Center ATTN: Tech Lib China Lake, CA 93555
3	Commander Naval Ordnance Station ATTN: F.W. Robbins S.E. Mitchell Tech Lib Indian Head, MD 20640
1	Director Lawrence Livermore National Laboratory ATTN: L355, A.C. Bunkingham P.O. Box 808 Livermore, CA 94550
1	Director Los Alamos Scientific Lab ATTN: D. Durak P.O. Box 1663 Los Alamos, NM 87544
1	Director Los Alamos Scientific Laboratory 1 ATTN: Group T-7, B. Wendroff Mail Stop 233, P.O. Box 1663 Los Alamos, NM 87544
1	Calspan Corporation ATTN: E.B. Fisher P.O. Box 400 Buffalo, NY 14225
1	Paul Gough Associates, Inc. ATTN: P.S. Gough 1048 South Street Portsmouth, NH 03801
2	Commandant US Army Infantry School ATTN: ATSH-CD-CSO-OR Fort Benning, GA 31905
1	AFWL/SUL Kirtland AFB, NM 87117

DISTRIBUTION LIST

No. of Copies	Organization
3	Scientific Research Associates, Inc. ATTN: H. McDonald R.C. Buggeln H.J. Gibeling P.O. Box 498 Glastonbury, CT 06033
1	Massachusetts Institute of Technology Department of Materials Science and Engineering ATTN: J. Szekely 77 Massachusetts Avenue Cambridge, MA 02139
1	New York University Graduate Center of Applied Sciences ATTN: M. Summerfield 26 36 Stuyvesant Street New York, NY 10053
1	Pennsylvania State University Department of Mechanical Engineering ATTN: K.K. Kuo University Park, PA 16802
1	Princeton University Guggenheim Laboratories Department of Aerospace and Mechanical Science ATTN: L.H. Caveny P.O. Box 710 Princeton, NJ 08540
1	Rensselaer Polytechnic Institute Mathematical Sciences Department ATTN: D. Drew Troy, NY 12181
1	University of Cincinnati ATTN: A. Hamed Cincinnati, OH 45221
1	University of Cincinnati Department of Aerospace Engineering ATTN: W. Tabakoff Cincinnati, OH 45221
1	University of Delaware Department of Mathematic Science ATTN: M.Z. Nashed Newark, DE 19711
1	University of Illinois College of Engineering Department of Aeronautical and Astronautical Engineering ATTN: H. Krier Urbana, IL 61801
1	University of Illinois-Urbana Mechanics and Industrial Engineering ATTN: S.L. Soo Urbana, IL 61801
1	University of Maryland Institute of Physical Sciences and Technology ATTN: S.I. Pai College Park, MD 20742
1	University of Wisconsin-Madison Mathematics Research Center ATTN: J.R. Bowen 1225 W. Dayton Street Madison, WI 53706
1	Worcester Polytechnic Institute Department of Mathematics ATTN: P.W. Davis Worcester, MA 01609

DISTRIBUTION LIST

No. of Copies	Organization
	Aberdeen Proving Ground
	Dir, USAMSAA
	ATTN: DRXSY-D
	DRXSY-MP, H. Cohen
	Cdr, USATECOM
	ATTN: DRSTE-TO-F
	Dir, MTD
	ATTN: STEAP-MT-A
	STEAP-MT-A
	STEAP-MT-G, C. Herud
	Cdr, CRDC, AMCCOM
	ATTN: DRSMC-CLB-PA
	DRSMC-CLN
	DRSMC-CLJ-L

USER EVALUATION OF REPORT

Please take a few minutes to answer the questions below; tear out this sheet, fold as indicated, staple or tape closed, and place in the mail. Your comments will provide us with information for improving future reports.

1. BRL Report Number _____

2. Does this report satisfy a need? (Comment on purpose, related project, or other area of interest for which report will be used.)

_____

_____

_____

3. How, specifically, is the report being used? (Information source, design data or procedure, management procedure, source of ideas, etc.) _____

_____

_____

4. Has the information in this report led to any quantitative savings as far as man-hours/contract dollars saved, operating costs avoided, efficiencies achieved, etc.? If so, please elaborate.

_____

_____

5. General Comments (Indicate what you think should be changed to make this report and future reports of this type more responsive to your needs, more usable, improve readability, etc.) _____

_____

_____

_____

6. If you would like to be contacted by the personnel who prepared this report to raise specific questions or discuss the topic, please fill in the following information.

Name: _____

Telephone Number: _____

Organization Address: _____

_____

_____